Solar chromospheric fine structures: dynamics and energetics

Kostas Tziotziou

RCAAM, Academy of Athens & National Observatory of Athens

The solar chromosphere

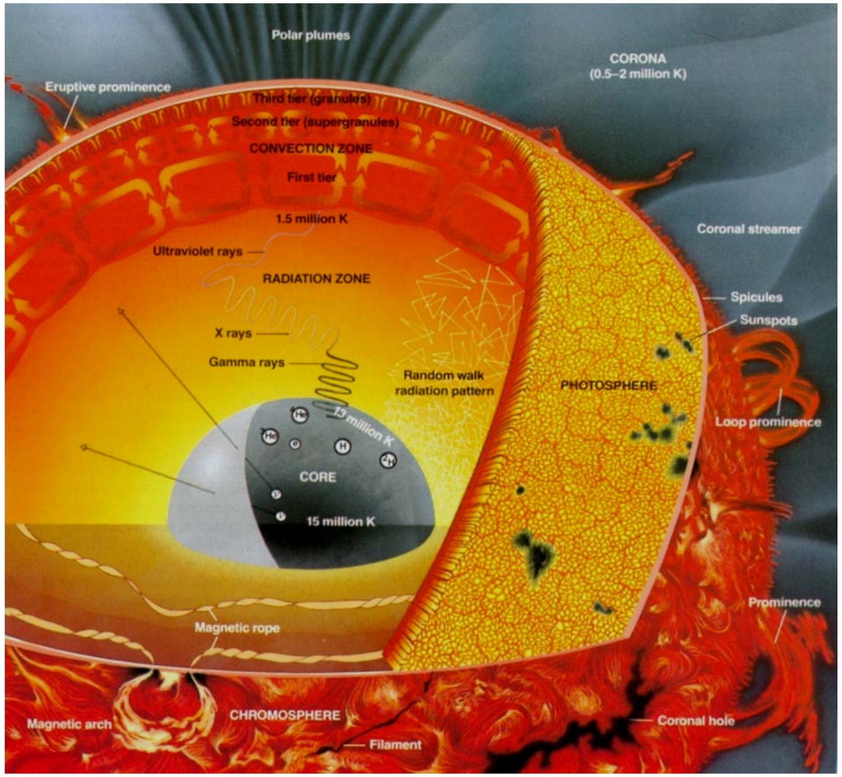

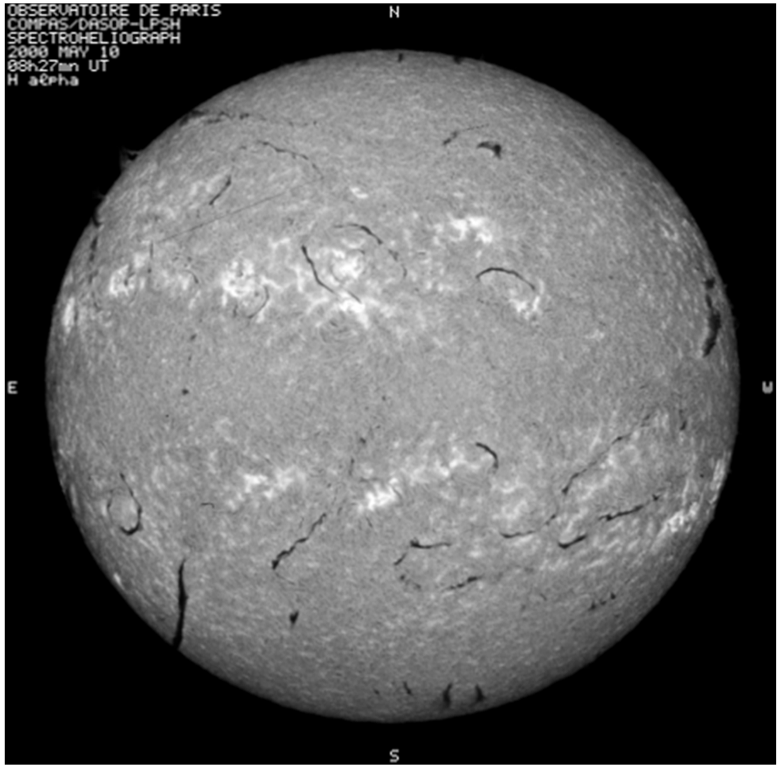

A thin layer above the photosphere where photons created deep at the radiation zone after passing through the convection zone finally escape free towards the upper atmospheric layers

The chromospheric network

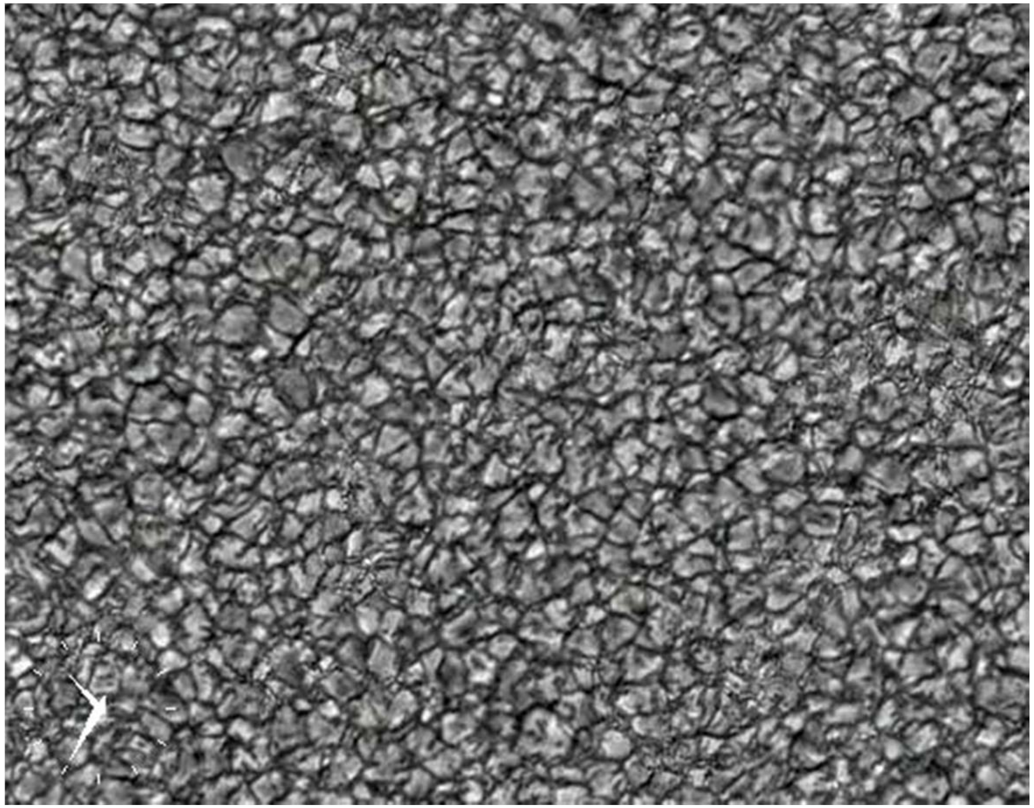

• photosheric granules are the top of convective flows. They have a typical length of 2 Mm and lifetime of ~16 min

• photospheric granulation leads to the formation of the chromosperic network

The chromospheric network

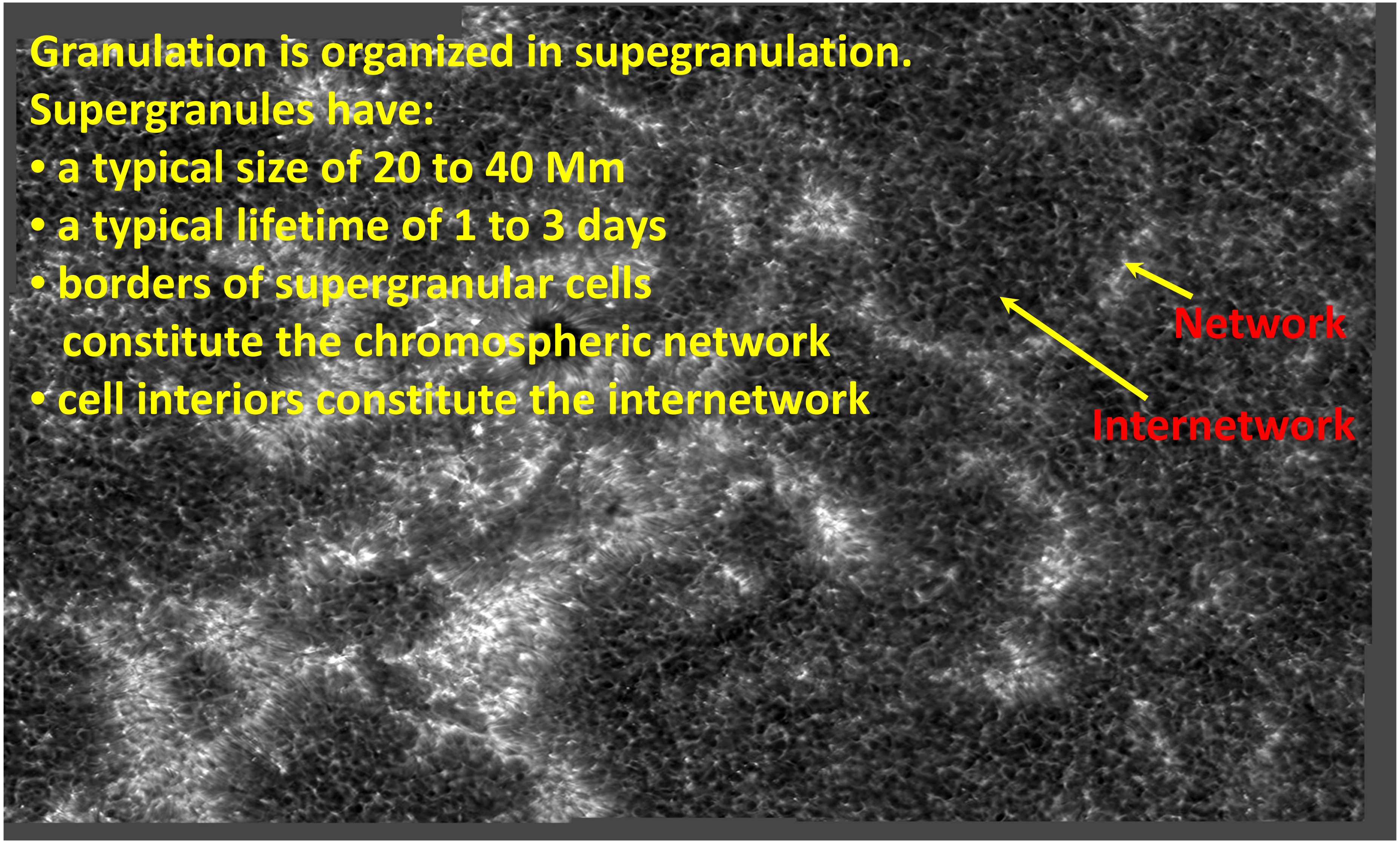

P-modes

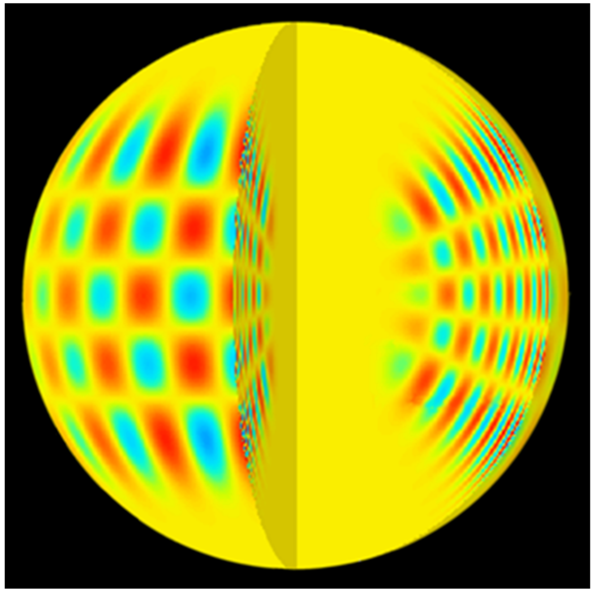

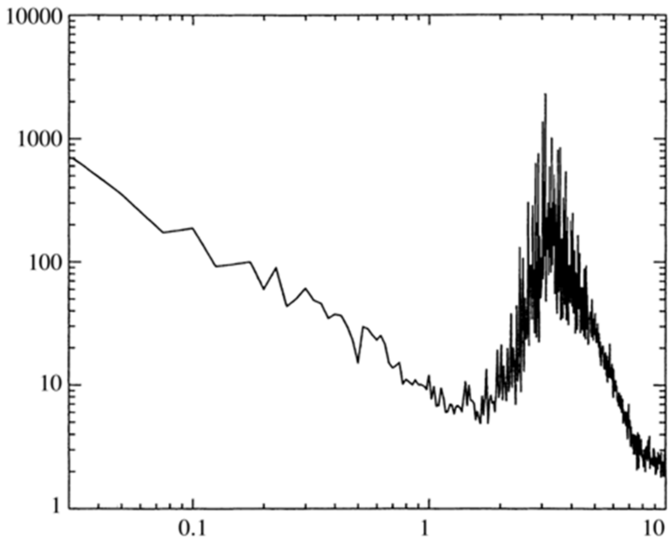

Turbulence in the convection zone can create acoustic power, i.e. waves that travel towards the photosphere.

P-mode or **acoustic** waves have pressure as their restoring force, hence the name "p-mode". Their dynamics are determined by the variation of the speed of sound inside the sun.

P-mode oscillations have frequencies > 1 mHz and are very strong in the 2-4 mHz range, where they are often referred to as "5-minute oscillations“ (~3.33 mHz)

P-modes are evanescent waves and the general belief was that can not propagate to higher atmospheric layers.

However this is not absolutely true!

Chromospheric magnetic fields

Chromospheric magnetic fields:

- more diffuse and weaker than the photospheric ones
- shows less internetwork structure
- shows more extensive regions of horizontal canopy fields which are closely related to chromospheric fibrils

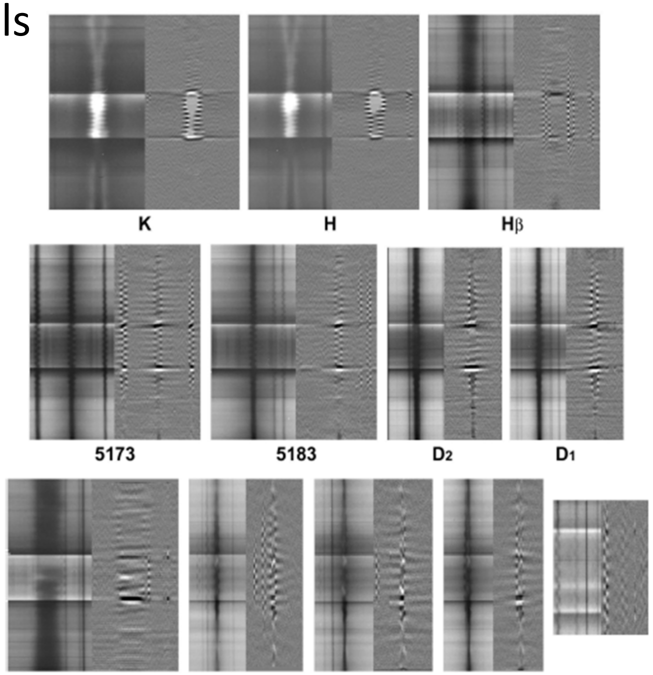

How do we observe them?

Ca H and K lines: good polarization sensitivity of their emission cores
Hβ wings: significantly blended with photospheric lines
Mg I 5173 and 5183 Å: well-behaved signals with 5173 giving a slightly
stronger response
D2: The red wing of the core contaminated by a water vapor line
D1: Good for ground observations
Hα: rather weak polarization signal even in the steep wings adjacent to its core; suffers from varying emission in the core which produces an opposites signed polarization signal; blended with a photospheric line in its red wing.
Ca II 8662 Å: seriously blended with a photospheric line
Ca II 8498 and 8542 Å: somewhat similar with the latter being stronger, less affected by blends and having a more symmetric core profile. The cores of both lines frequently show emission that produces complicated Stokes profiles
10830 Å multiplet : has the advantage of being formed almost entirely in the chromosphere but it varies greatly in strength from place to place

Harvey, 2009, ASPC 405, 157

Chromospheric magnetic fields

The magnetic flux of the quiet Sun internetwork

- the quiet IN regions are pervaded by horizontal magnetic flux
- transverse flux is almost x 5 the longitudinal flux
- The vertical fields are concentrated in the intergranular lanes
- the stronger horizontal fields are somewhat separated spatially from the vertical fields and mostly occur at the edges of the bright granules

B^L

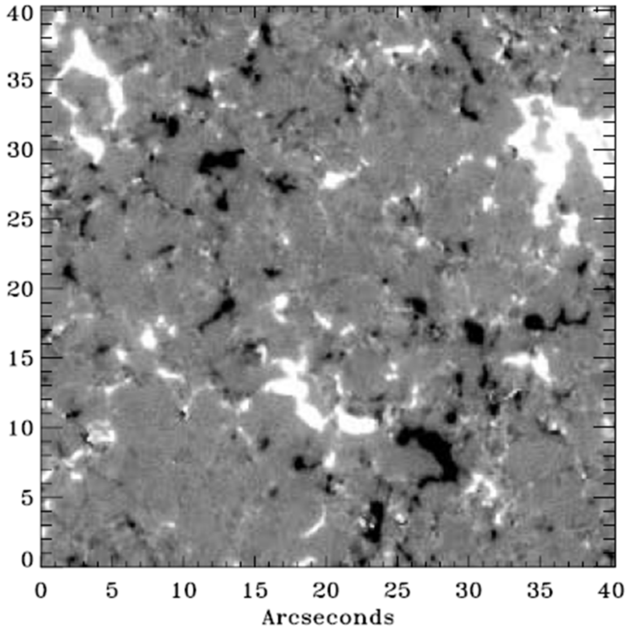

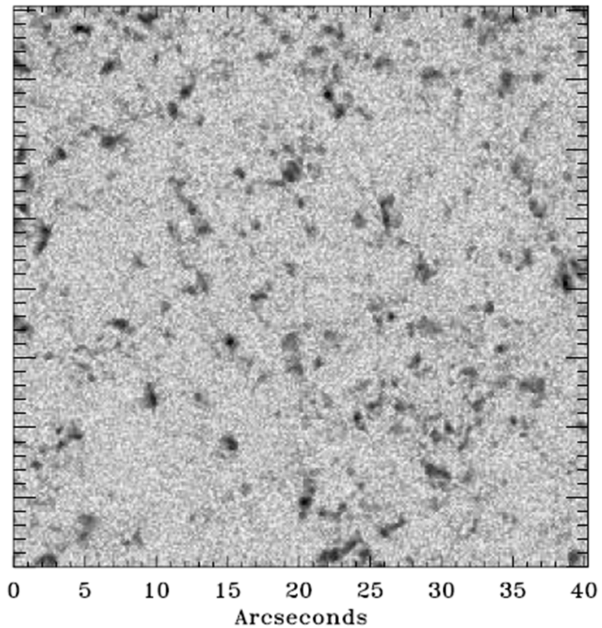

B^T

LITES ET AL. THE ASTROPHYSICAL JOURNAL, 672:1237–1253, 2008 January 10

Chromospheric magnetic fields

Small-scale magnetic flux emergence in quiet Sun

Two photospheric lines Fe I 630.25 nm and Fe I 630.15 nm with SP of SOT

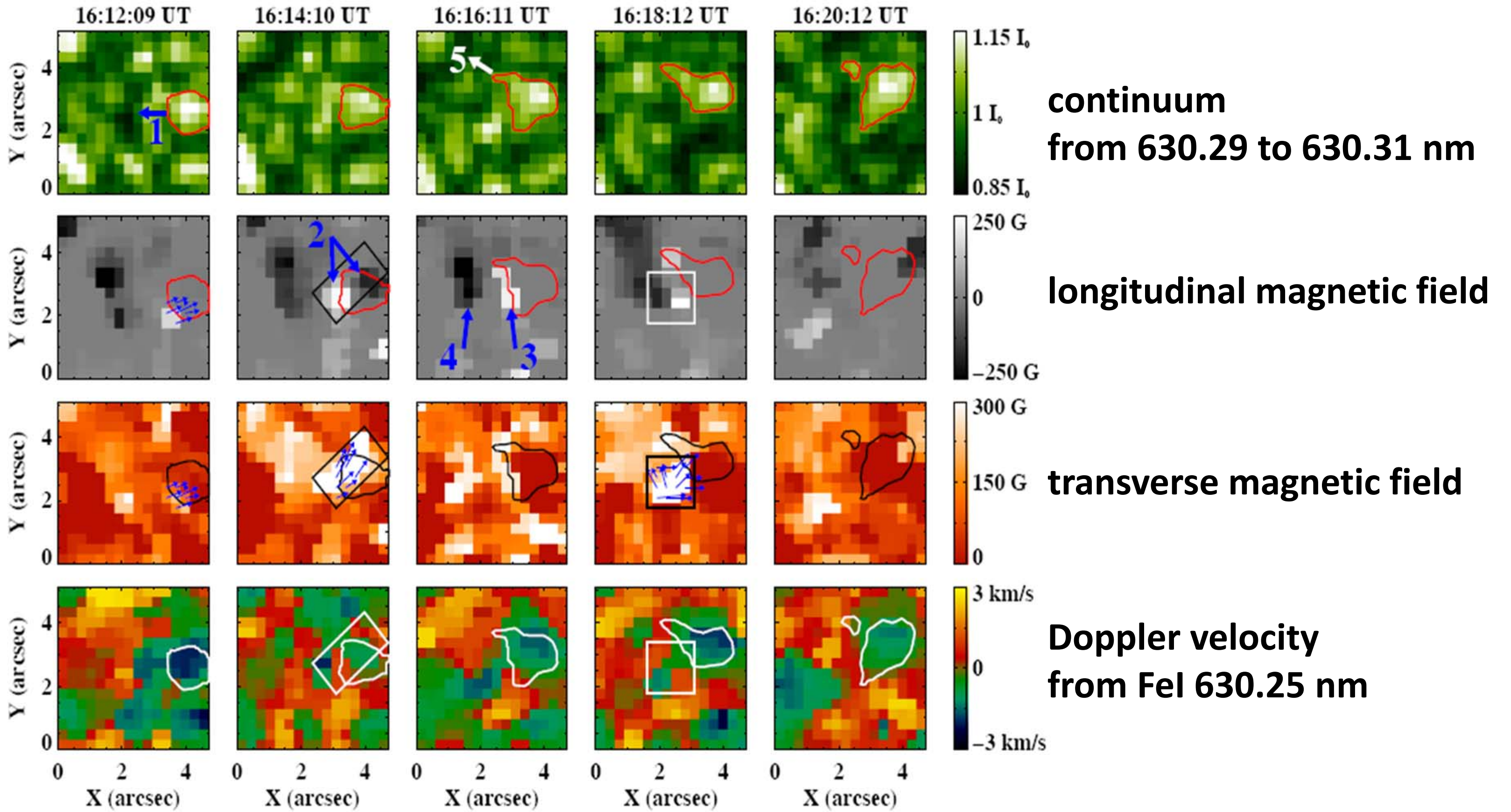

J. Zhang, S. H. Yang & C. L. Jin
Research in Astron. Astrophys. **2009** Vol. **9** No. **8**, 921 – 932

Chromospheric magnetic fields

Emergence of vertical magnetic fields above quiet sun granules with typical lifetime of the order of 20 min

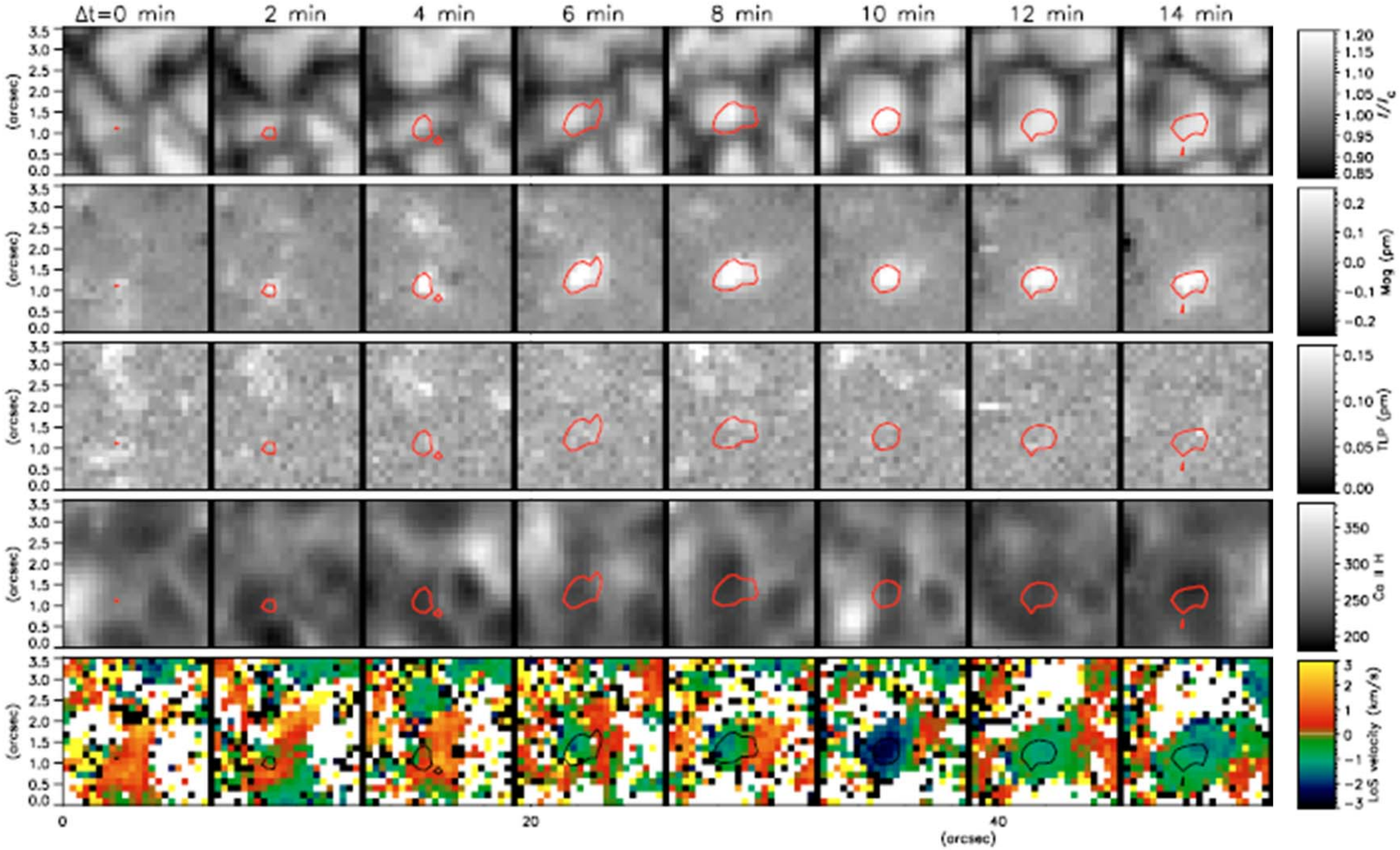

D. Orozco Suárez et al. A&A 481, L33–L36 (2008)

Chromospheric magnetic fields

Emergence of small-scale magnetic loops

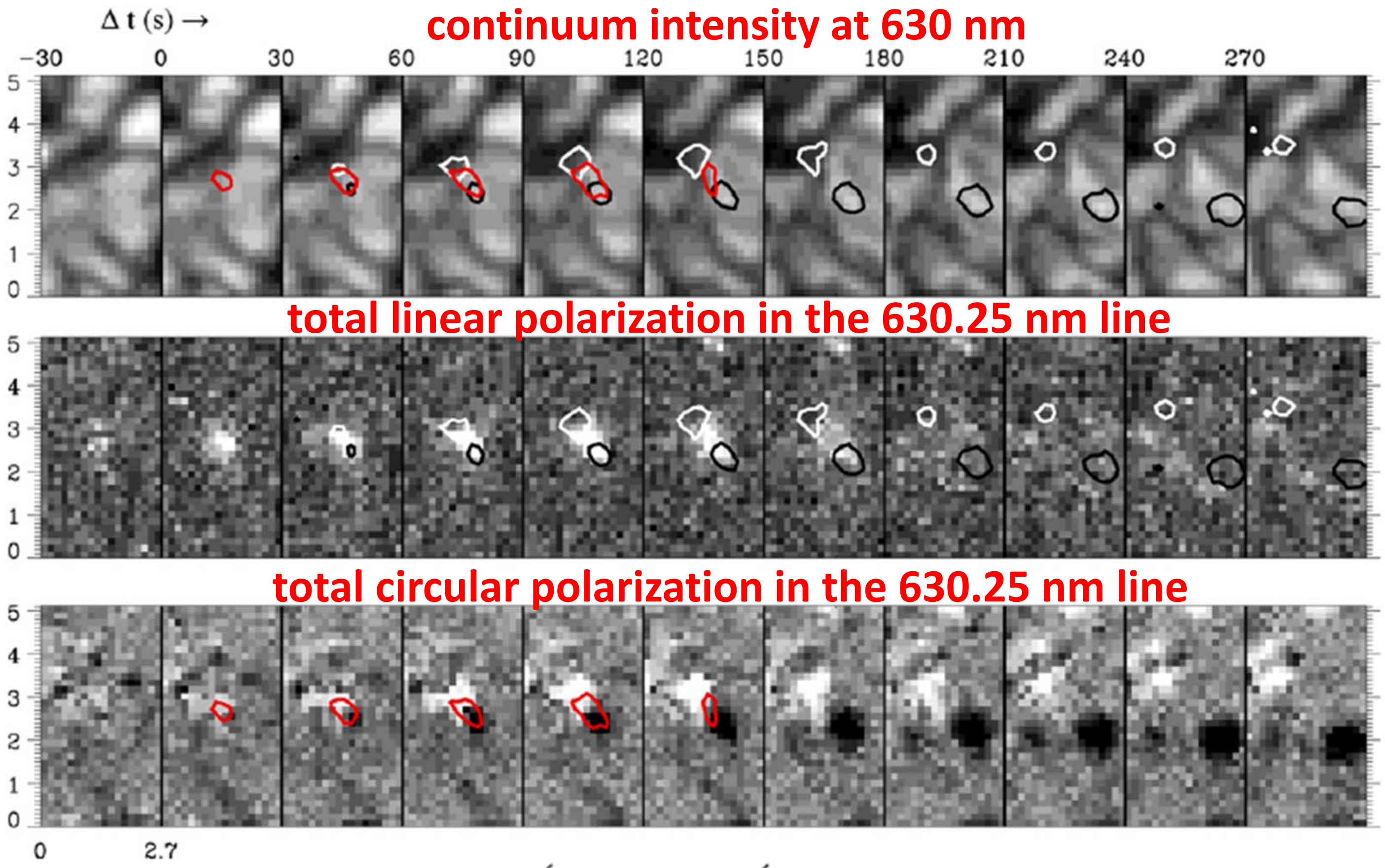

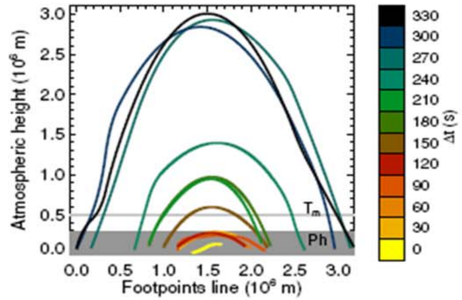

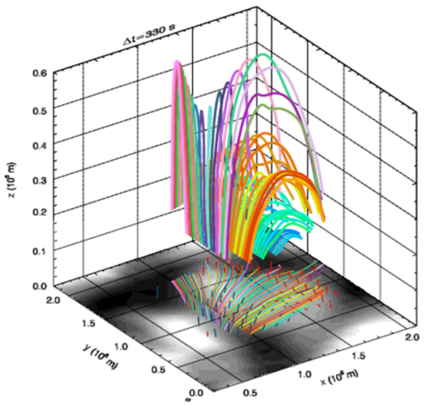

MARTÍNEZ GONZÁLEZ & BELLOT RUBIO
THE ASTROPHYSICAL JOURNAL, 700:1391–1403, 2009 August 1

Chromospheric magnetic fields

Magnetic elements in internetwork

G-band

Ca II H

Fe I Magnetogram

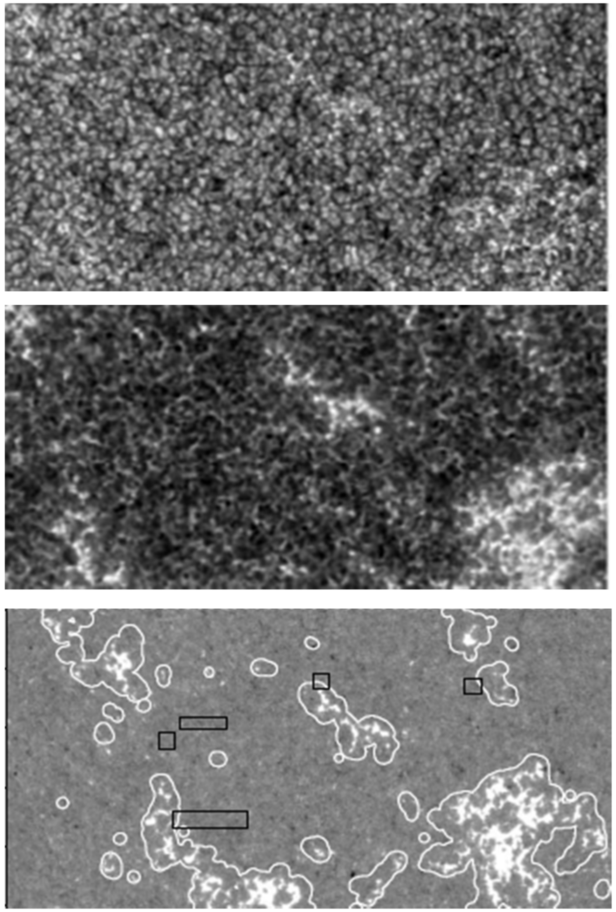

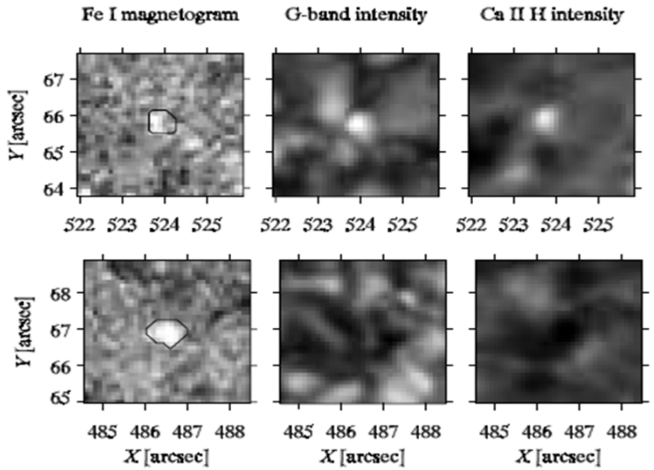

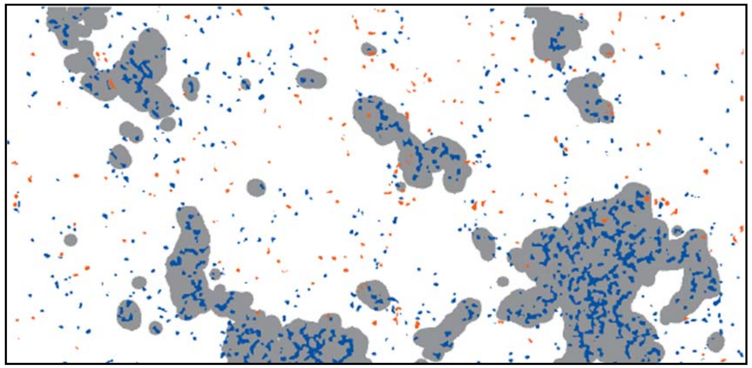

Sample mask of magnetic elements:
positive flux are blue, negative flux are red

DE WIJN ET AL. The Astrophysical Journal, 684:1469–1476, 2008 September 10

Chromospheric magnetic fields

Magnetic elements in internetwork

Histograms of the velocity of IMEs toward the network boundary measured over 35 s (left) and 597 s (right).

Blue: positive polarity
Red: negative polarity

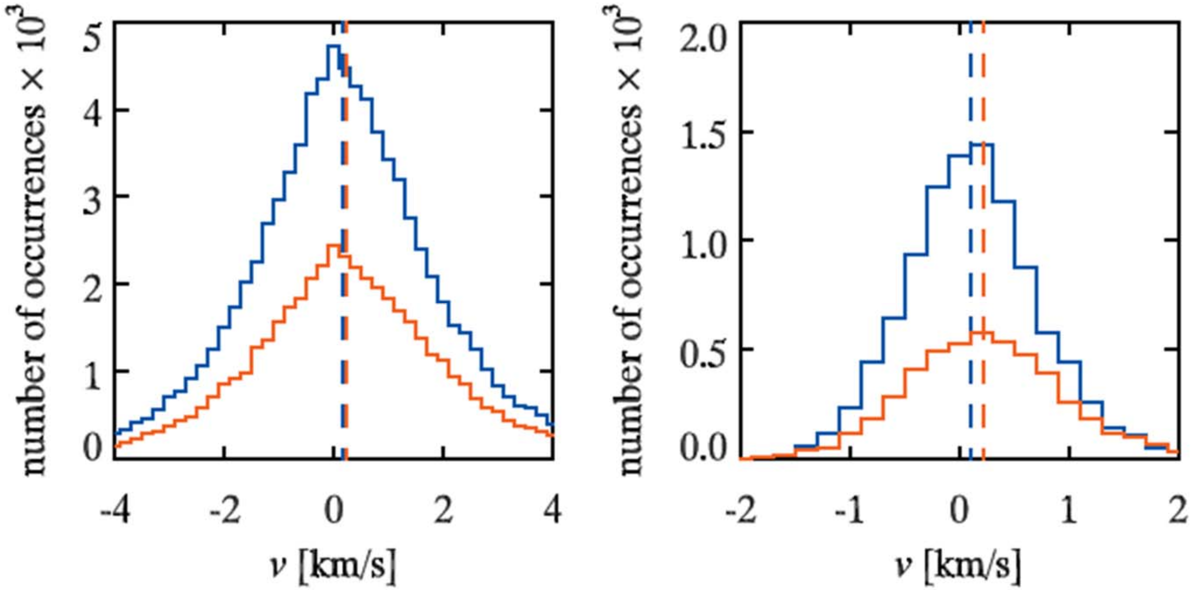

The apparent flows indicate a bias of about 0.2 km/s toward the network boundary. Elements of negative polarity show a higher bias than elements of positive polarity, perhaps as a result of the dominant positive polarity of the network in the field of view or because of increased mobility due to their smaller size.

DE WIJN ET AL. The Astrophysical Journal, 684:1469–1476, 2008 September 10

Chromospheric magnetic fields

Supergranulation and network Formation

Using floating corks advected by velocity fields inferred from photometry measurements, Roudier et al. showed that long-living Trees of Fragmenting Granules play a crucial role in the advection of small-scale magnetic fields and in the build-up of the magnetic network

Corks and longitudinal magnetic field location after 24h (left) and 48h (right)

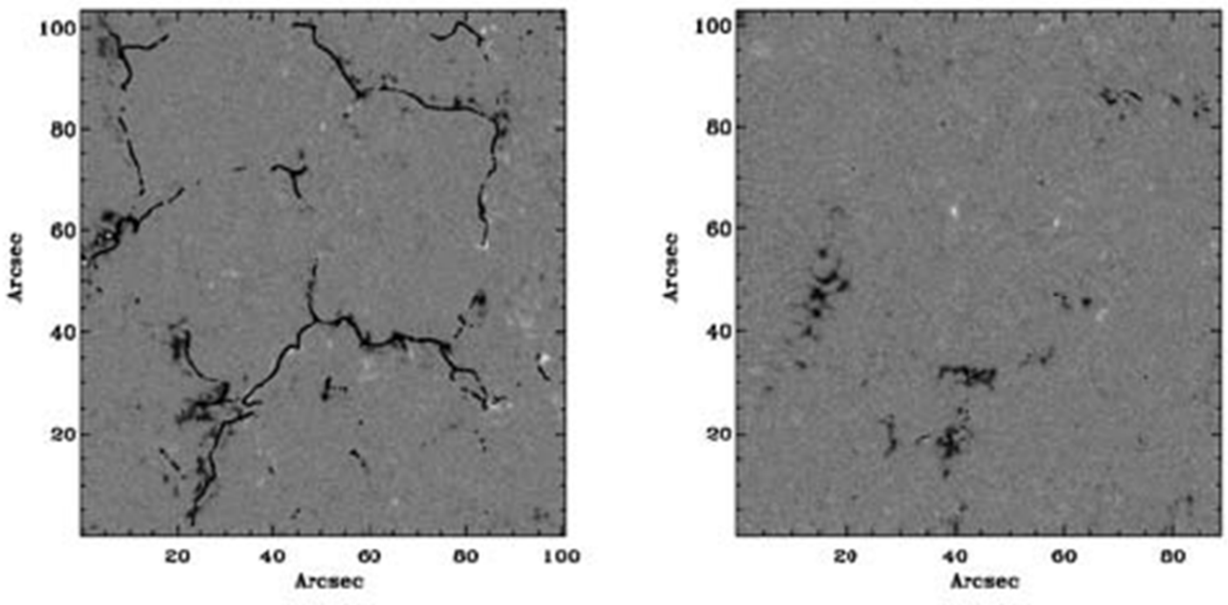

Roudier etal., 2009, A&A 495, 945

The chromospheric network

31 hours of SOHO/MDI magnetograms

H. Potts (Glasgow University, 2006)

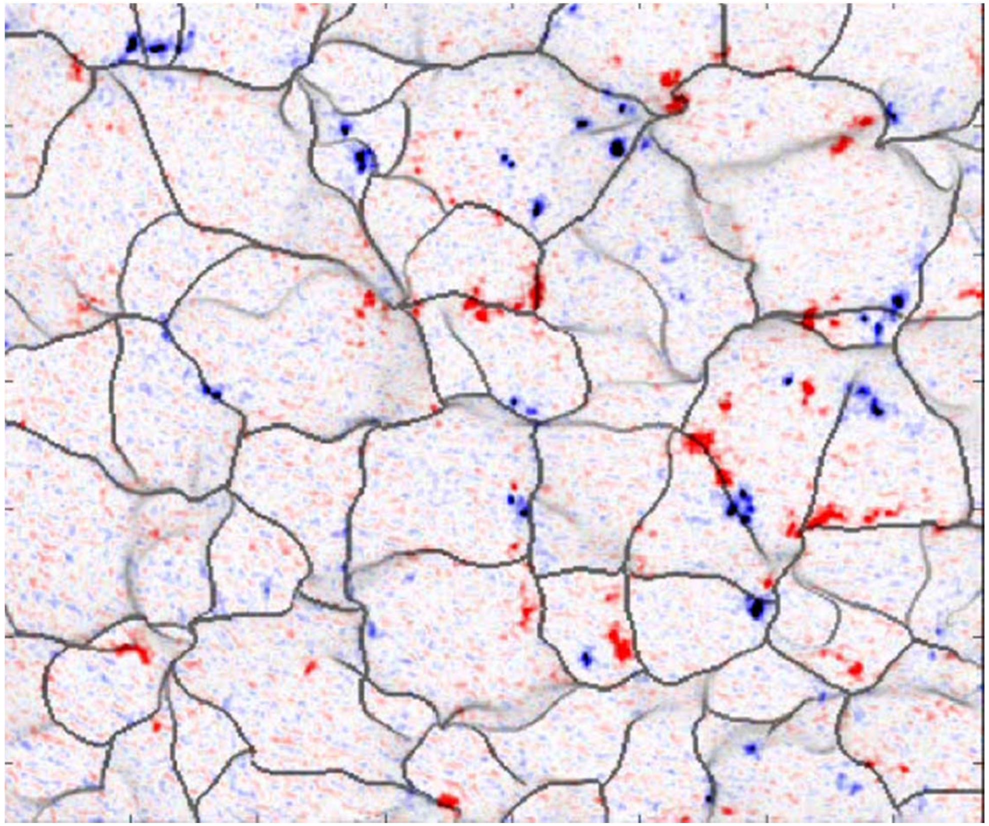

Majority of observed fine scale chromospheric structures reside at network boundaries

Fine scale structures (on-disc picture)

DOT observations

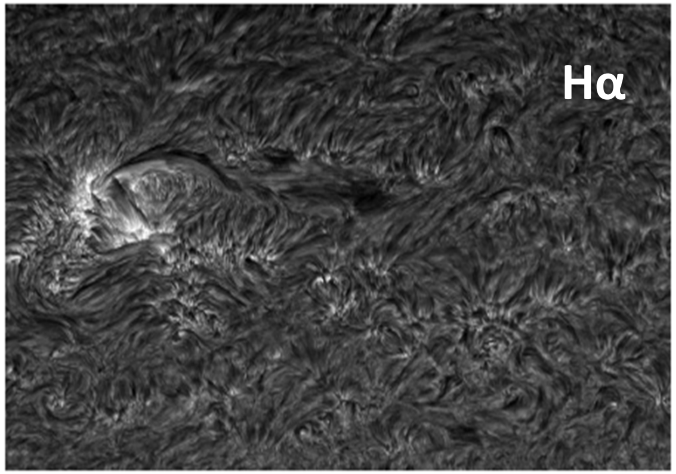

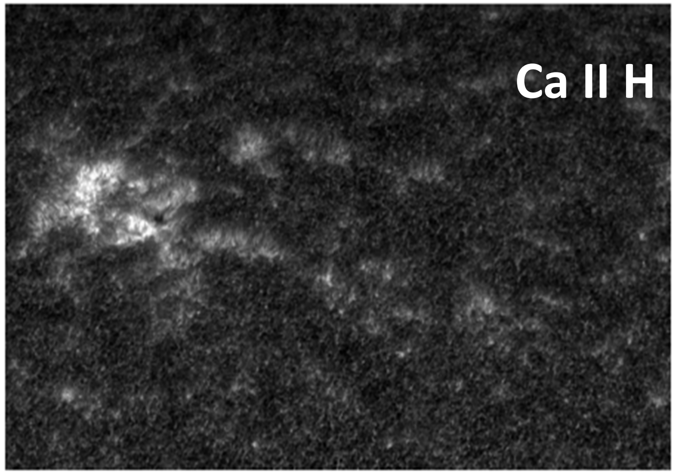

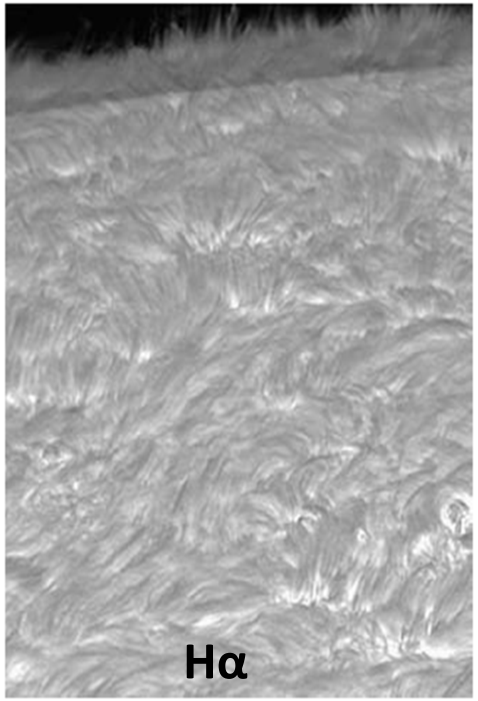

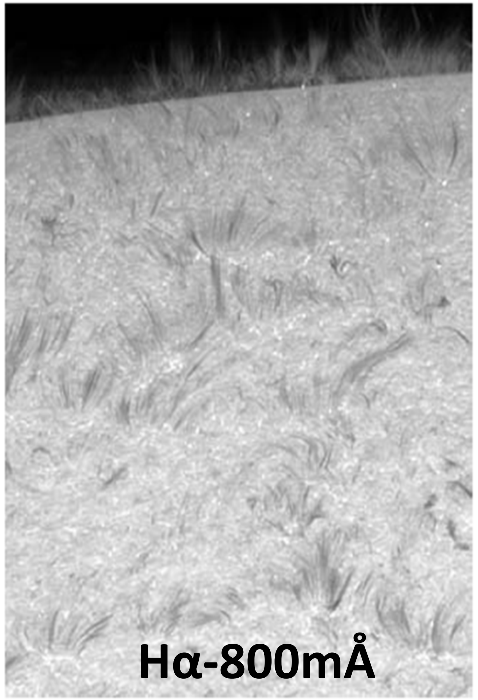

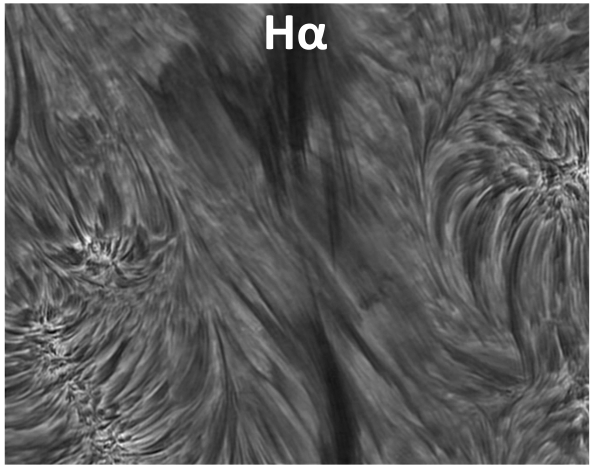

Rosette

Chain

Fine scale structures (on-disc picture)

Hα with CRISP@SST

Hα-0.6 Å

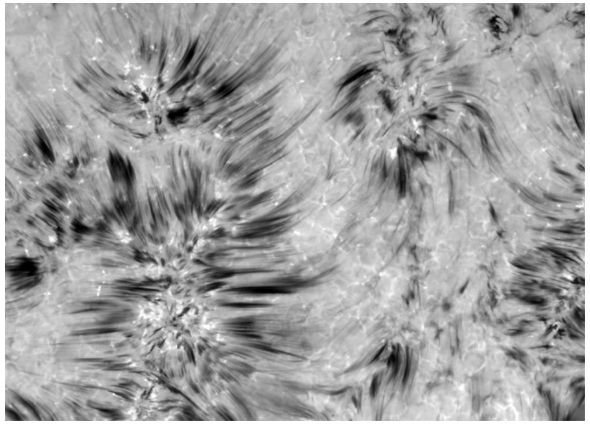

Hα line core

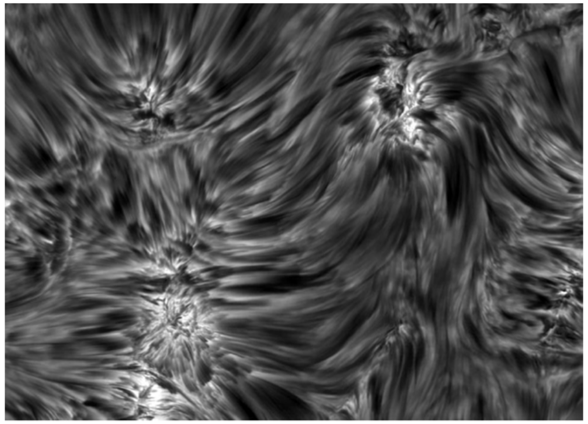

Hα+0.6 Å

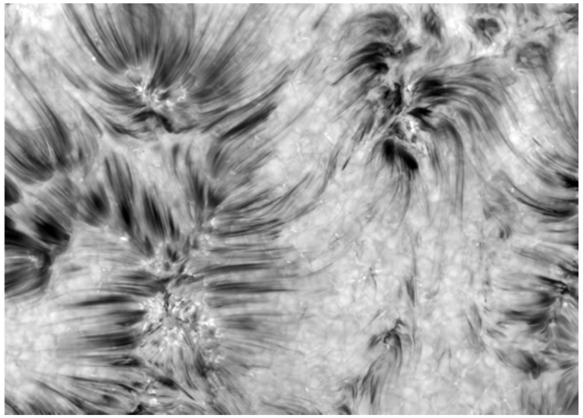

Quiet sun features: **mottles**

Active region features (plages, sunspots): **fibrils**

In general mottles and fibrils are:

- **jet-like structures**
- **～10000 km long**
- **～1000 km wide**
- **cool ～12000 K**

Fine scale structures (limb picture)

Ca II H HINODE/SOT observations

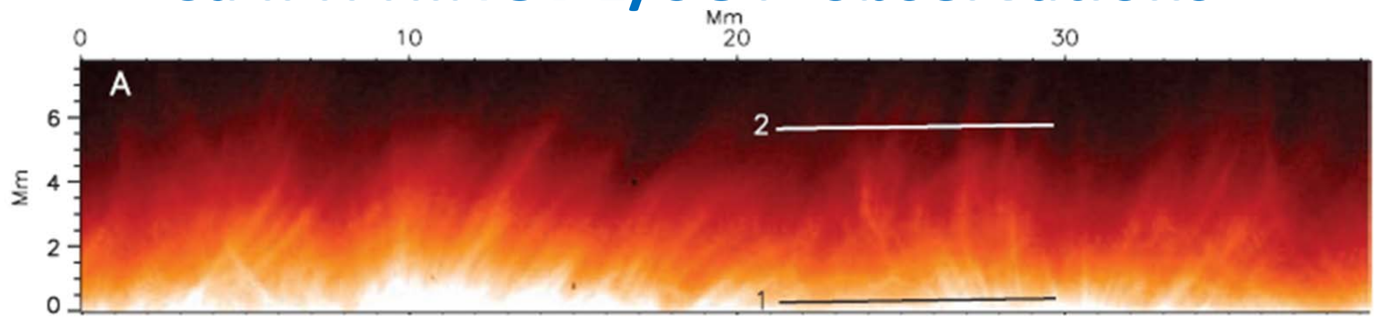

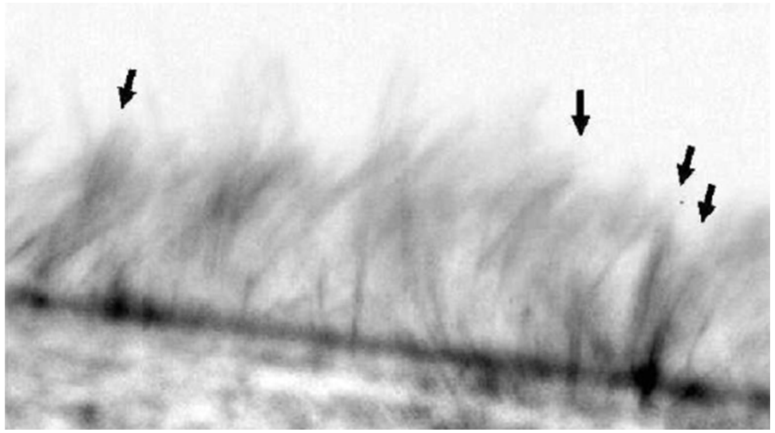

Spicules: jet-like structures seen at the limb. Associated to mottles and fibrils

Fine scale structures: dynamic jet-like flows

Ca II H with DOT

AR 10486

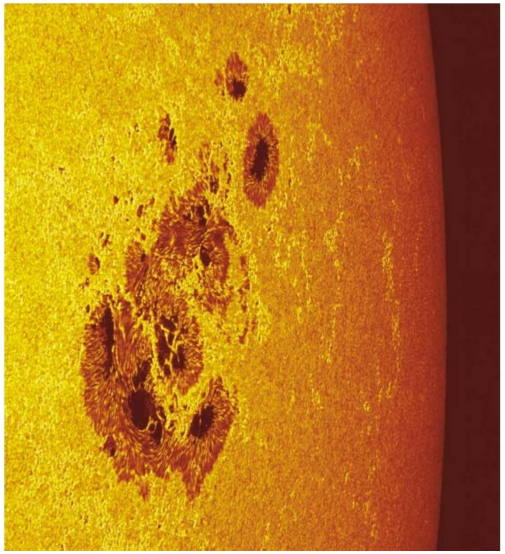

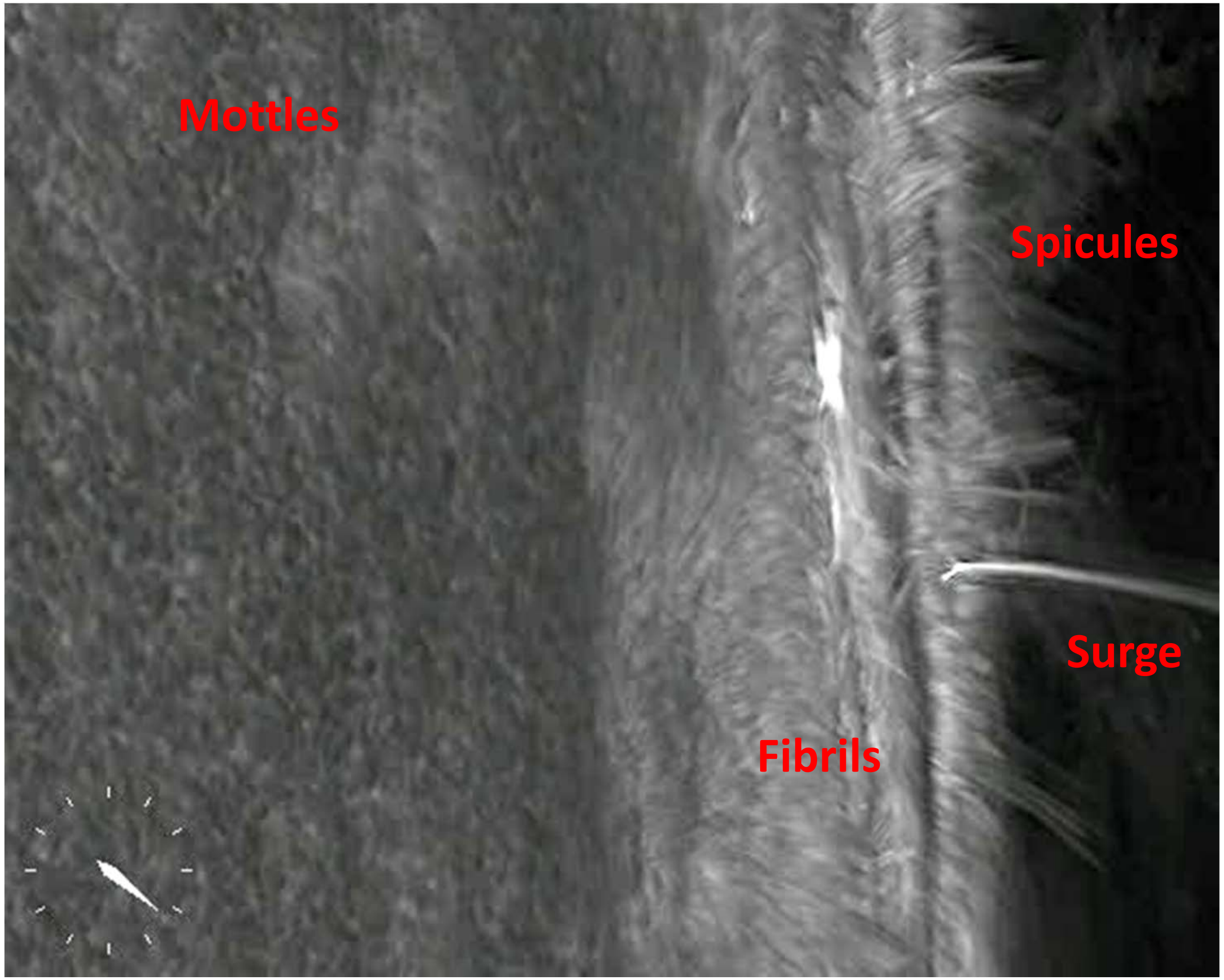

Spicules: two types?

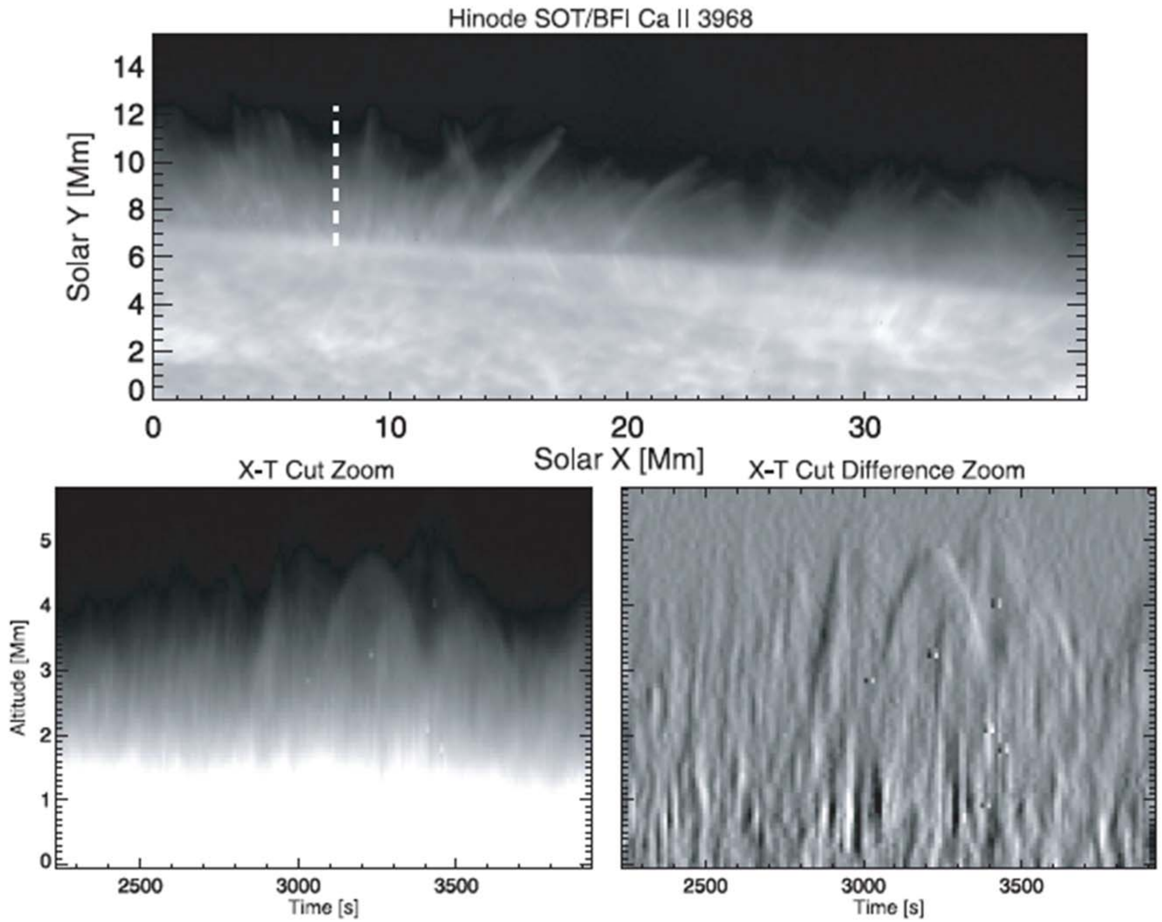

Short-lived vertical stripes and longer-lived parabolic paths

De Pontieu et al. **PASJ:** Publ. Astron. Soc. Japan **59**, S655–S662, 2007 November 30

Spicules: two types?

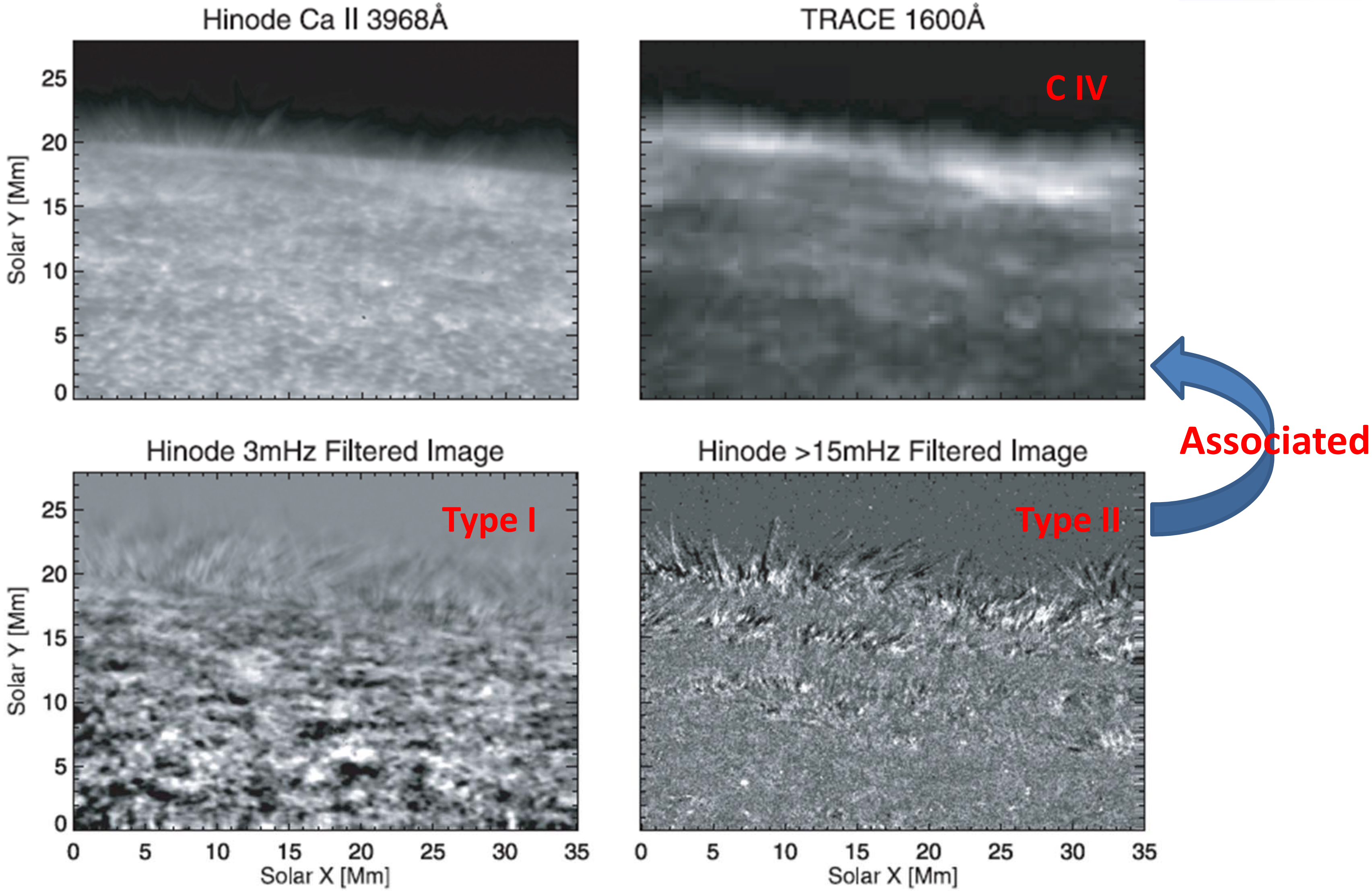

De Pontieu et al. **PASJ:** Publ. Astron. Soc. Japan **59**, S655–S662, 2007 November 30

Spicules: two types?

Type I

Type II

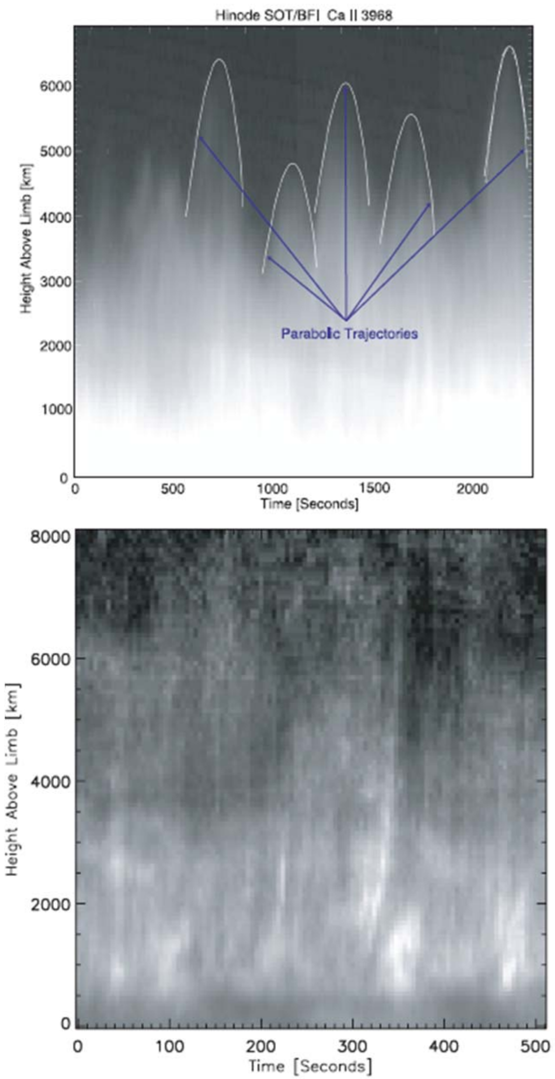

Type II spicules

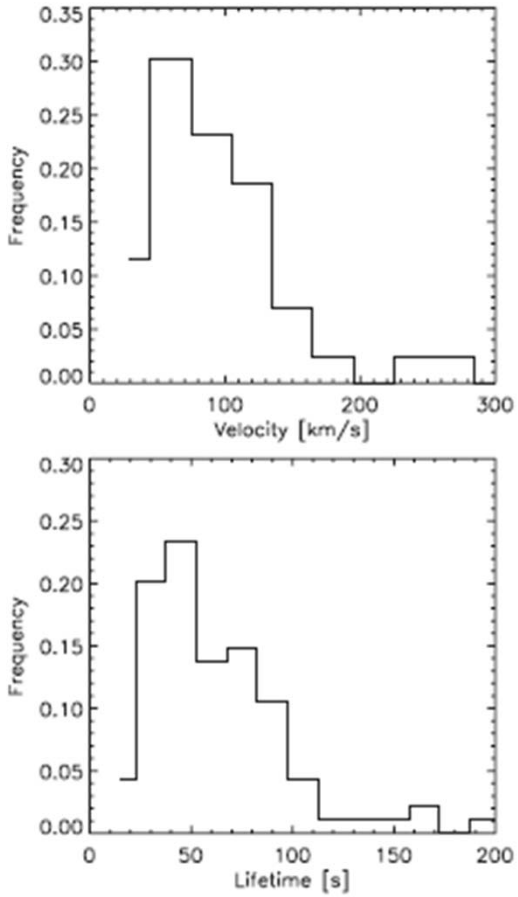

Type I:
- longer-lived 3-5 min
- velocities 10-50 km/s

Type II:
- short-lived 10-100s
- velocities 40-150 km/s

De Pontieu et al. **PASJ:** Publ. Astron. Soc. Japan **59**, S655–S662, 2007 November 30

On-disk counterparts of Type II spicules

Rapid blueshifted events (RBEs) with CRISP

Temporal cadence 6.7 s

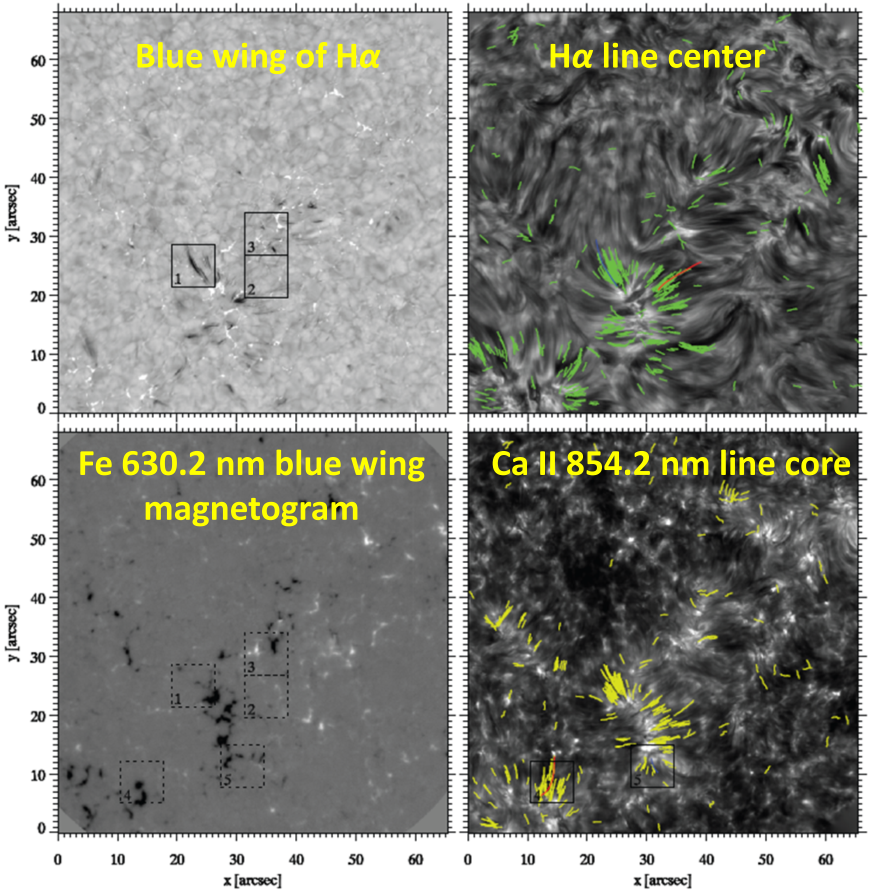

Hα

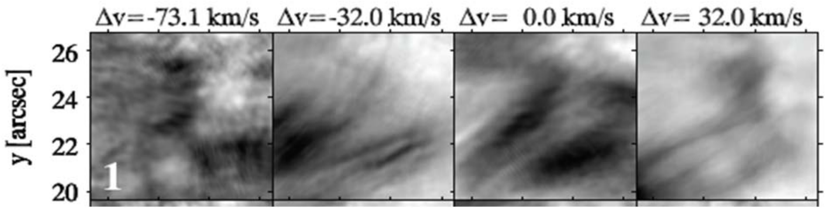

Ca II

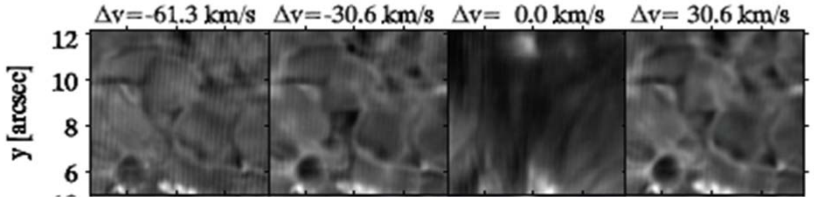

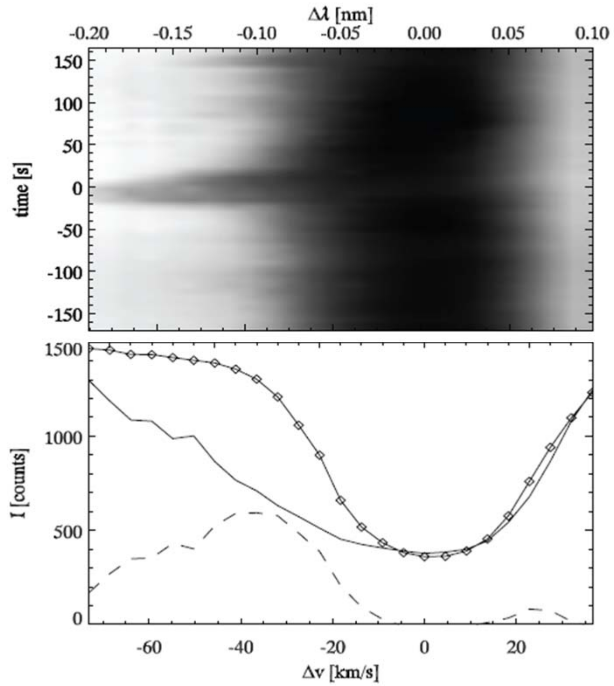

ROUPPE VAN DER VOORT ET AL.
THE ASTROPHYSICAL JOURNAL, 705:272–284, 2009 November 1

On-disk counterparts of Type II spicules

608 Hα RBEs (solid line)
413 Ca II 854.2 nm RBEs (dashed line)

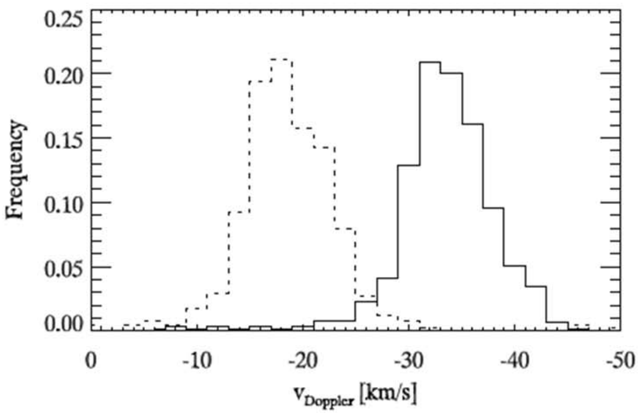

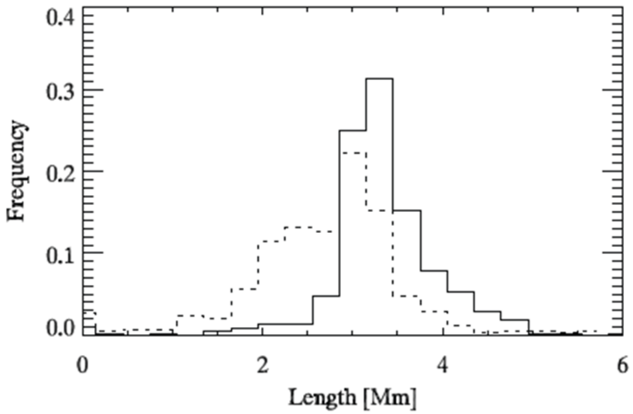

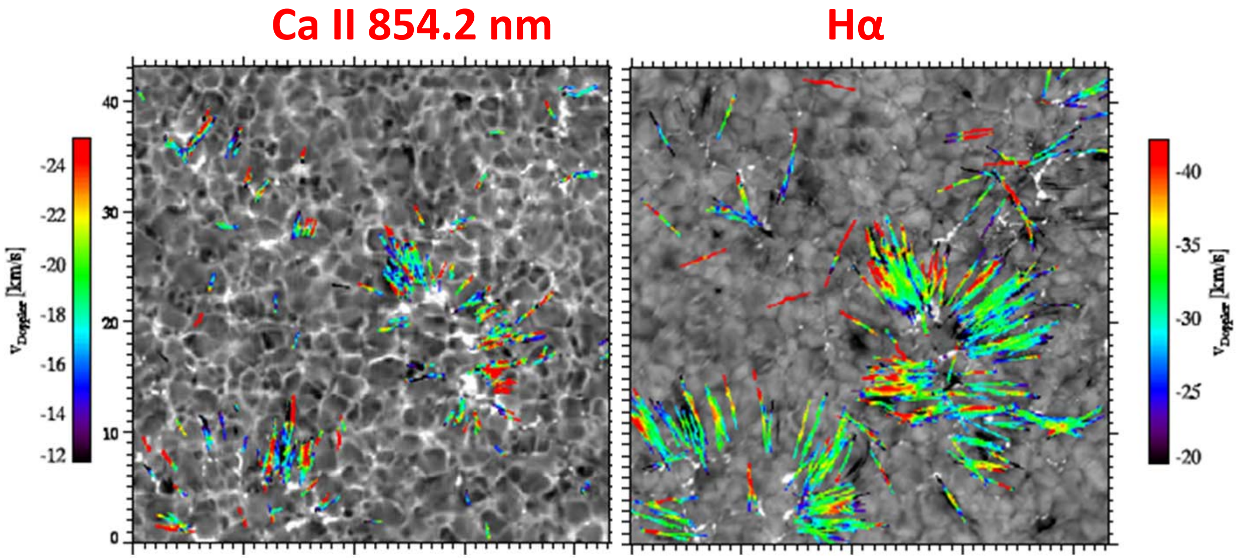

Transverse displacement and transverse velocity of 35 Hα RBEs

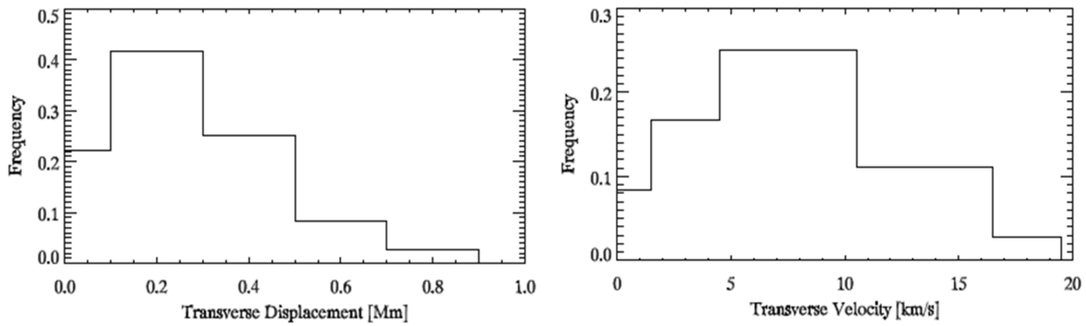

Similar to what De Pontieu et al. 2007 observed in Type II spicules at the limb

ROUPPE VAN DER VOORT ET AL.
THE ASTROPHYSICAL JOURNAL, 705:272–284, 2009 November 1

Where are high velocities in disc Type II spicules?

Spatial extent, lifetime, and location of RBEs near network suggest a link to type II spicules, however, the magnitude of the measured Doppler velocity is significantly lower than apparent motions seen at the limb.

Ca II 854.2 nm with IBIS

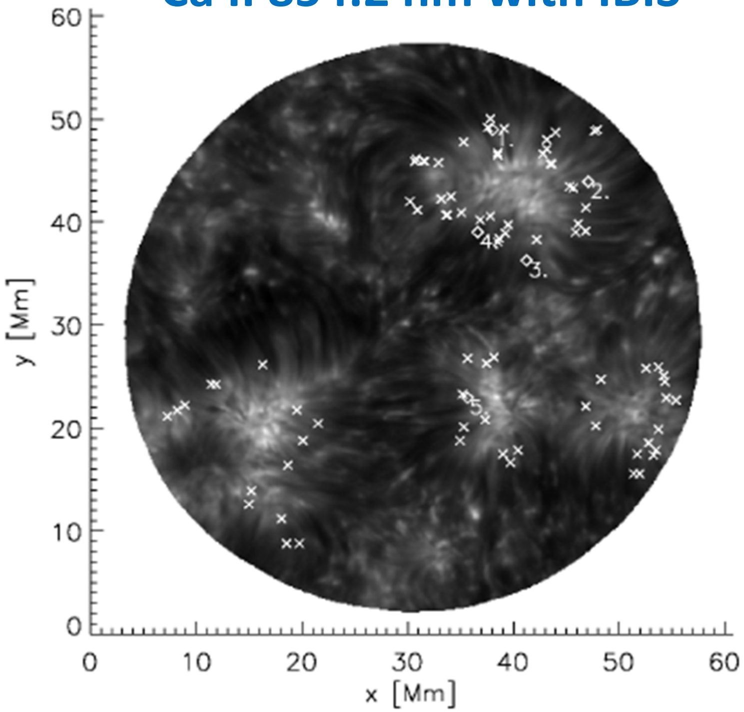

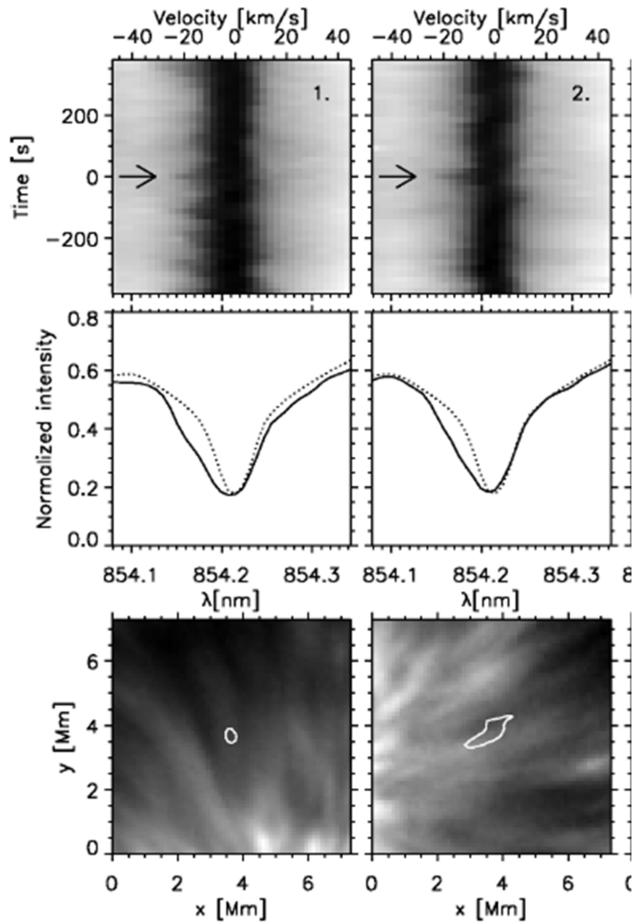

LANGANGEN ET AL. THE ASTROPHYSICAL JOURNAL, 679: L167–L170, 2008 June 1

Where are high velocities in disc Type II spicules?

LANGANGEN ET AL.
THE ASTROPHYSICAL JOURNAL, 679: L167

Monte Carlo simulations show that the visibility on the disk of high-velocity flows in RBEs is limited by a combination of line-of-sight projection and reduced opacity in upward propelled plasma.

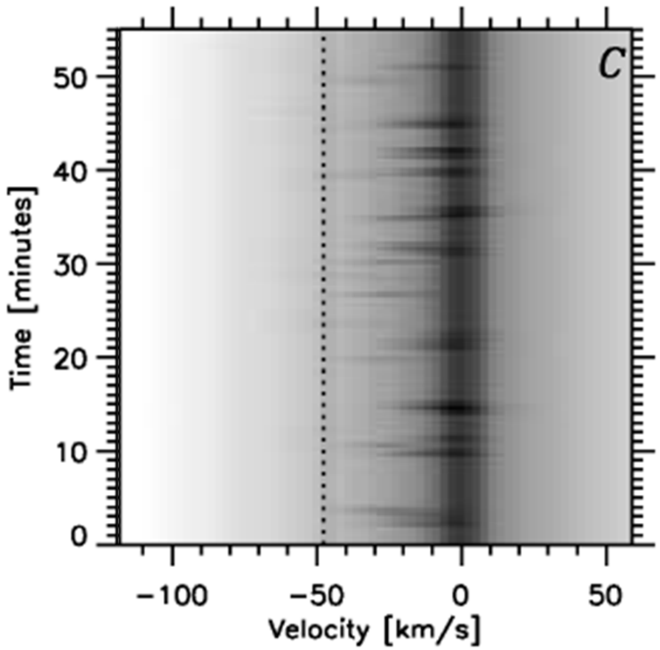

Simulations have shown that the chromospheric disc counterparts depend on location of null point with respect to the line height formation

Chromospheric null point

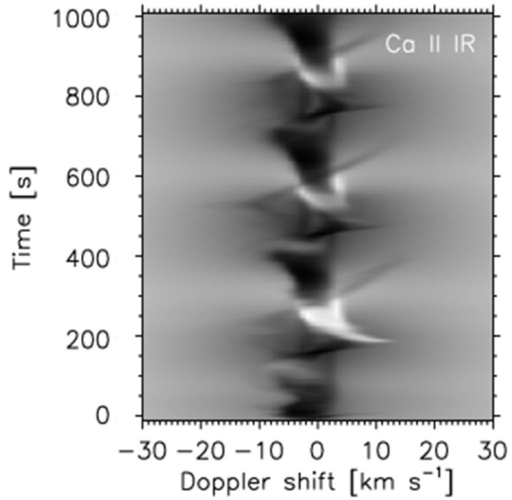

High null point

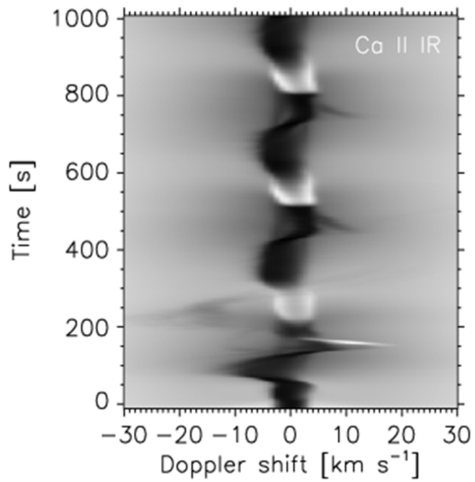

HEGGLAND, DE PONTIEU, & HANSTEEN
THE ASTROPHYSICAL JOURNAL, 702:1–18, 2009 September 1

The complete picture of chromospheric "fine" physics

Intricate and poorly understood physics and dynamics with significant impact on higher solar layers

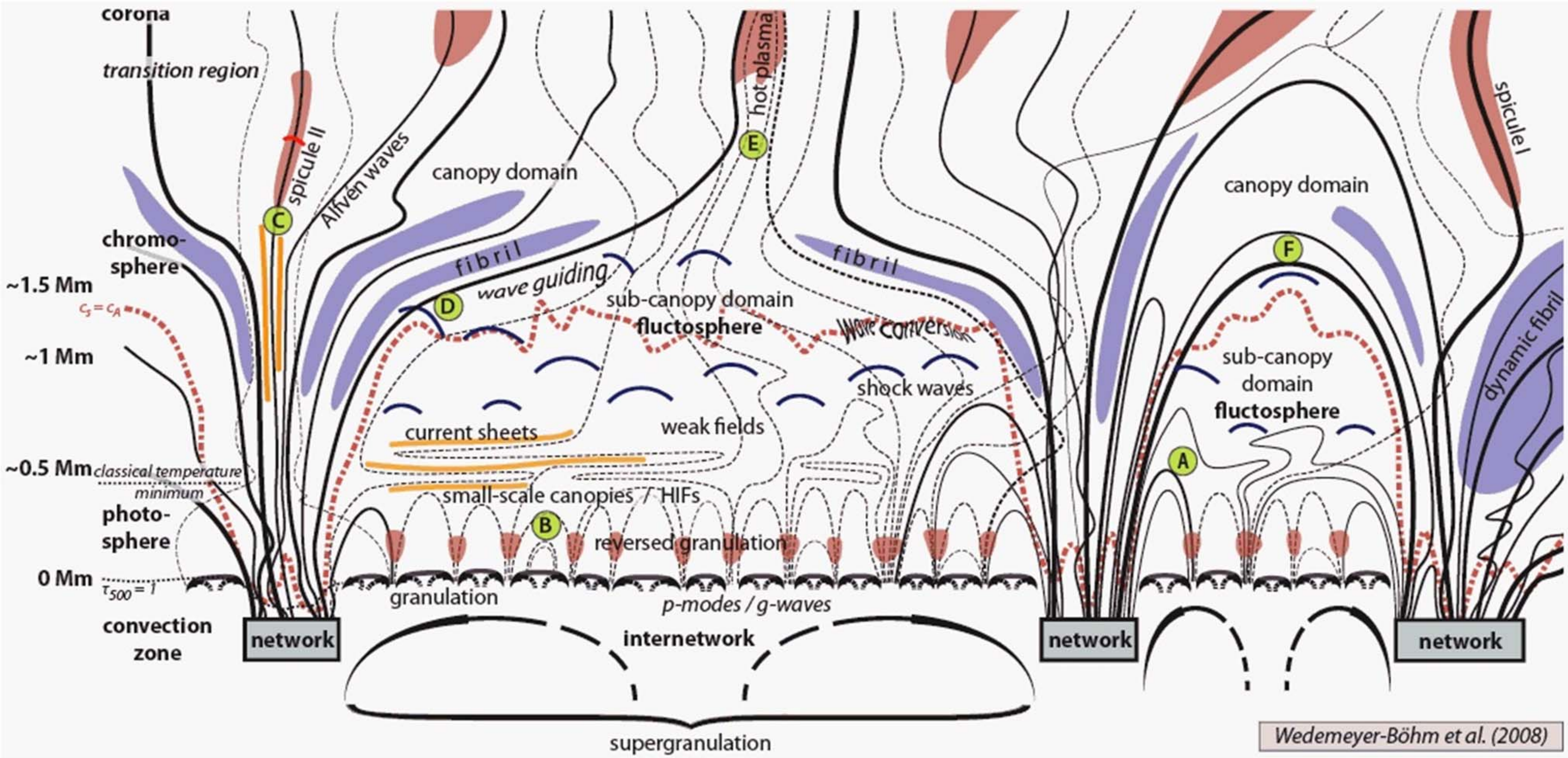

Obtaining physical properties with cloud model

Assuming:

➢optically thin structures laying above the photosphere

➢constant source function

Initial parameters:

- $\upsilon=0$
- $\Delta\lambda_D = 0.3$ Å
- $\tau_{max}= 1$
- $S = 0.155+0.159\times(P_1-C_1)/C_1$

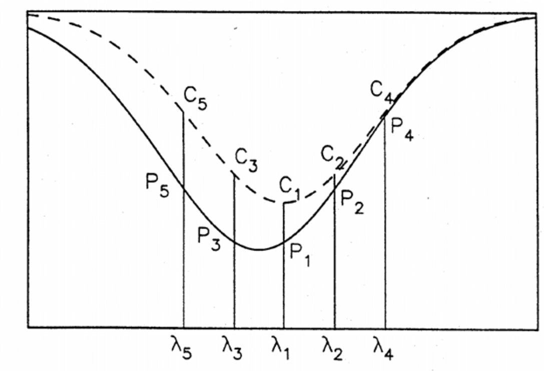

$$P_n = S + (C_n - S) \times exp(-\tau_n)$$

$$\tau_n = \tau_{\max} \cdot exp\left[-\left(\frac{\lambda_n - \lambda_1 - \lambda_1 \frac{v}{c}}{\Delta\lambda_D}\right)^2\right]$$

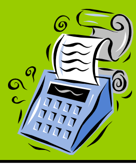

Iterative χ^2 fitting

i.e. 300 iterations

τ_{max}, υ, $\Delta\lambda_D$, S
that describe the observed profile

Obtaining physical properties with cloud model

+ general equations

$$
\begin{aligned}
\Delta\lambda_{\mathrm{D}} &= \frac{\lambda_0}{c}\sqrt{\frac{2kT}{m_H}+\xi_t^2} \\
N_2 &= 7.26\,10^7\frac{\tau_0\Delta\lambda_{\mathrm{D}}}{d} \\
N_e &= 3.2\,10^8\,\sqrt{N_2} \\
N_H &= 5\,10^8\,10^{0.5\log N_2} \\
p &= k(N_e+1.0851\,N_H)T_e \\
M &= (N_H m_H + 0.0851\,N_H \times 3.97\,m_H)\,d \\
\rho &= \frac{M}{d}
\end{aligned}
$$

Obtaining physical properties with cloud model

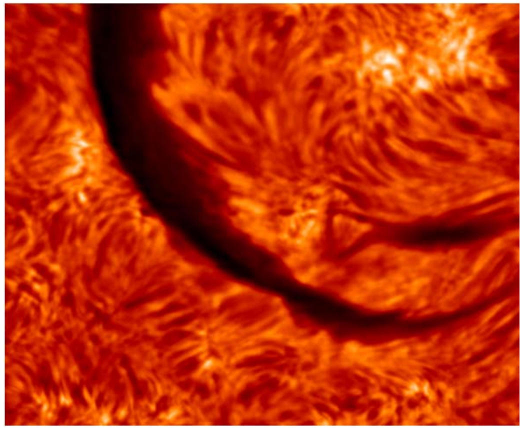

K. Tziotziou[1], G. Tsiropoula[1], and P. Mein[2]
A&A 402, 361–372 (2003)

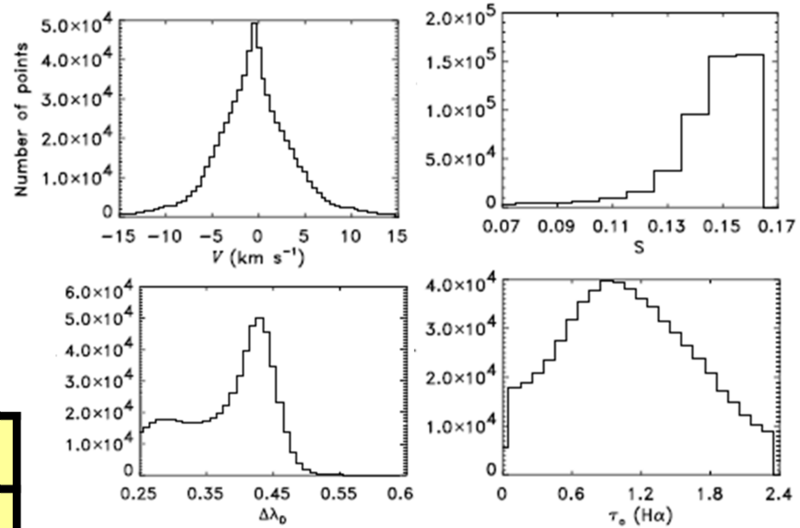

Parameters	*Average values*
N_2	$4.2\ 10^4$ cm^{-3}
N_H	$9.9\ 10^{10}$ cm^{-3}
N_e	$6.4\ 10^{10}$ cm^{-3}
m	$2.2\ 10^{-5}$ g cm^{-2}
ρ	$2.2\ 10^{-13}$ g cm^{-3}
T (for ξ_t=15 km/sec)	$1.0\ 10^4$ K
p (for ξ_t=15 km/sec)	0.24 dyn cm^{-2}
L	10 Mm
d	1 Mm
υ_{LOS}	15 km/sec

G. Tsiropoula[1] and K. Tziotziou[2]
A&A 424, 279–288 (2004)

Spicules: characteristics

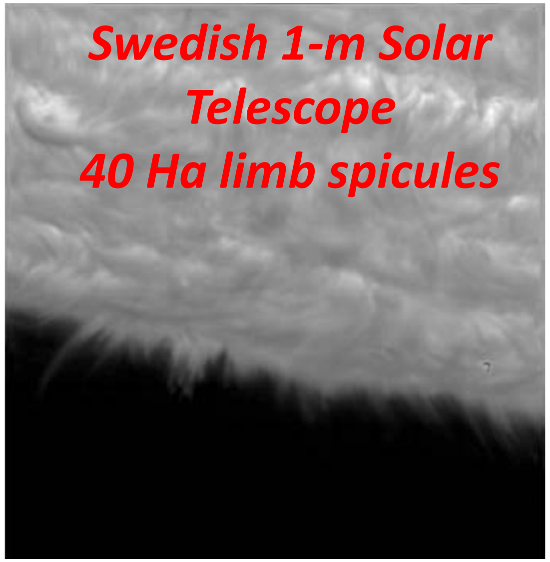

J.M. Pasachoff *et al.*
Solar Phys (2009) 260: 59

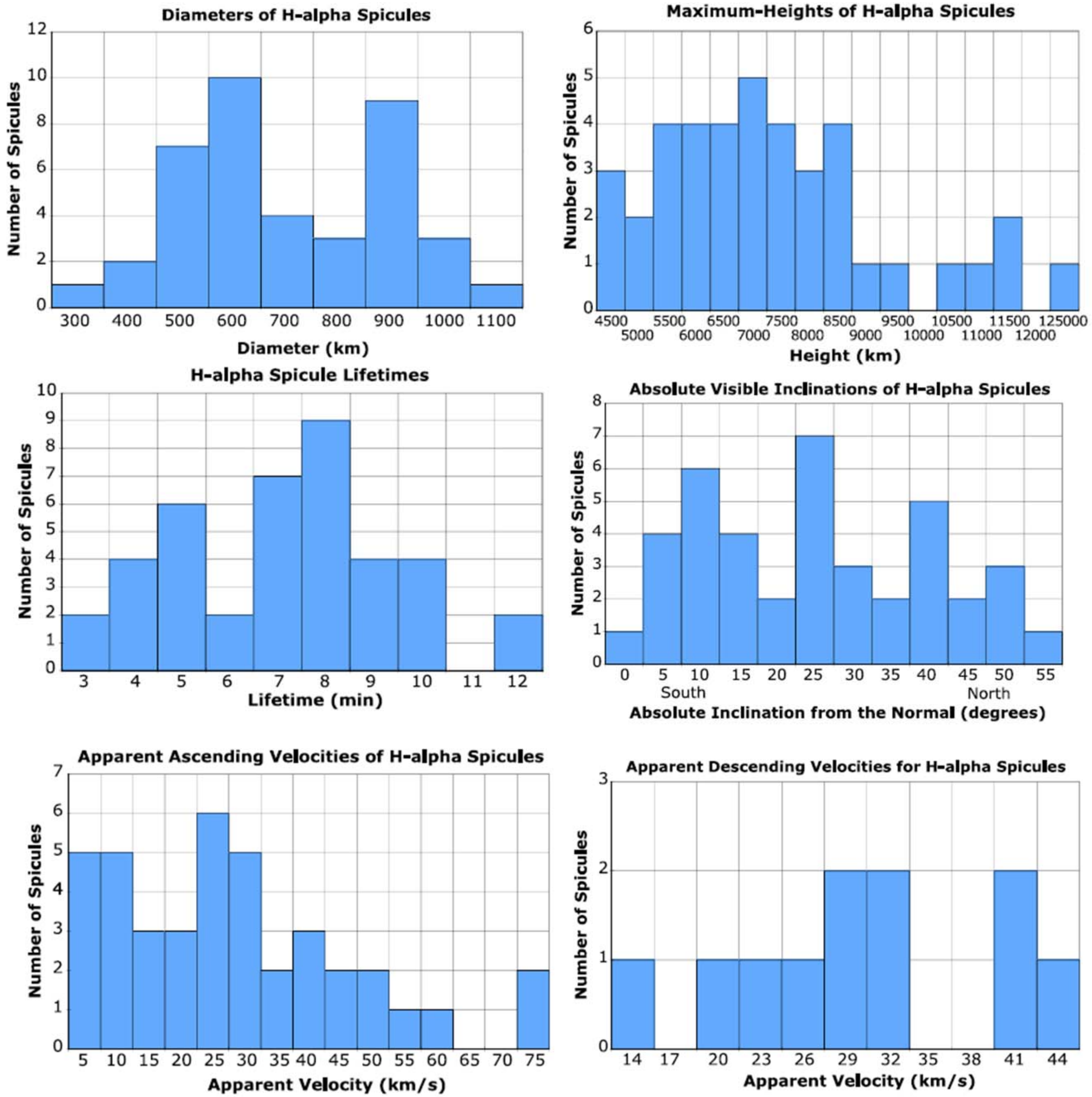

Dynamic fibrils in plage: characteristics

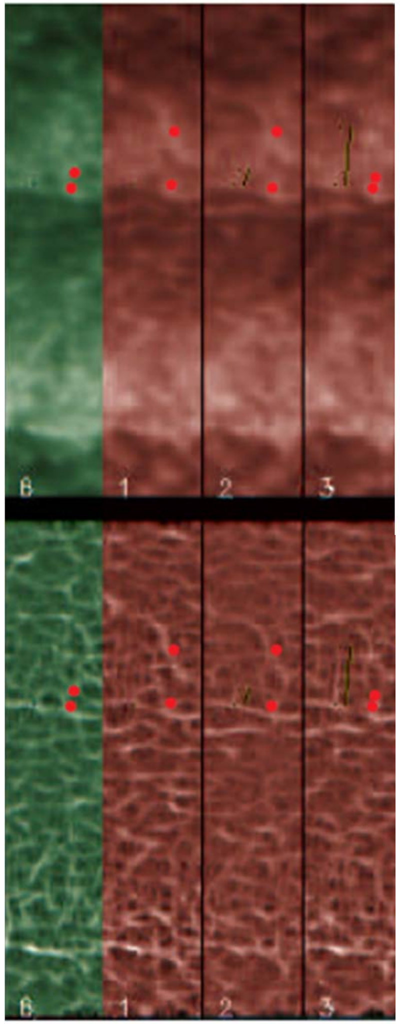

Anan et al. 2010

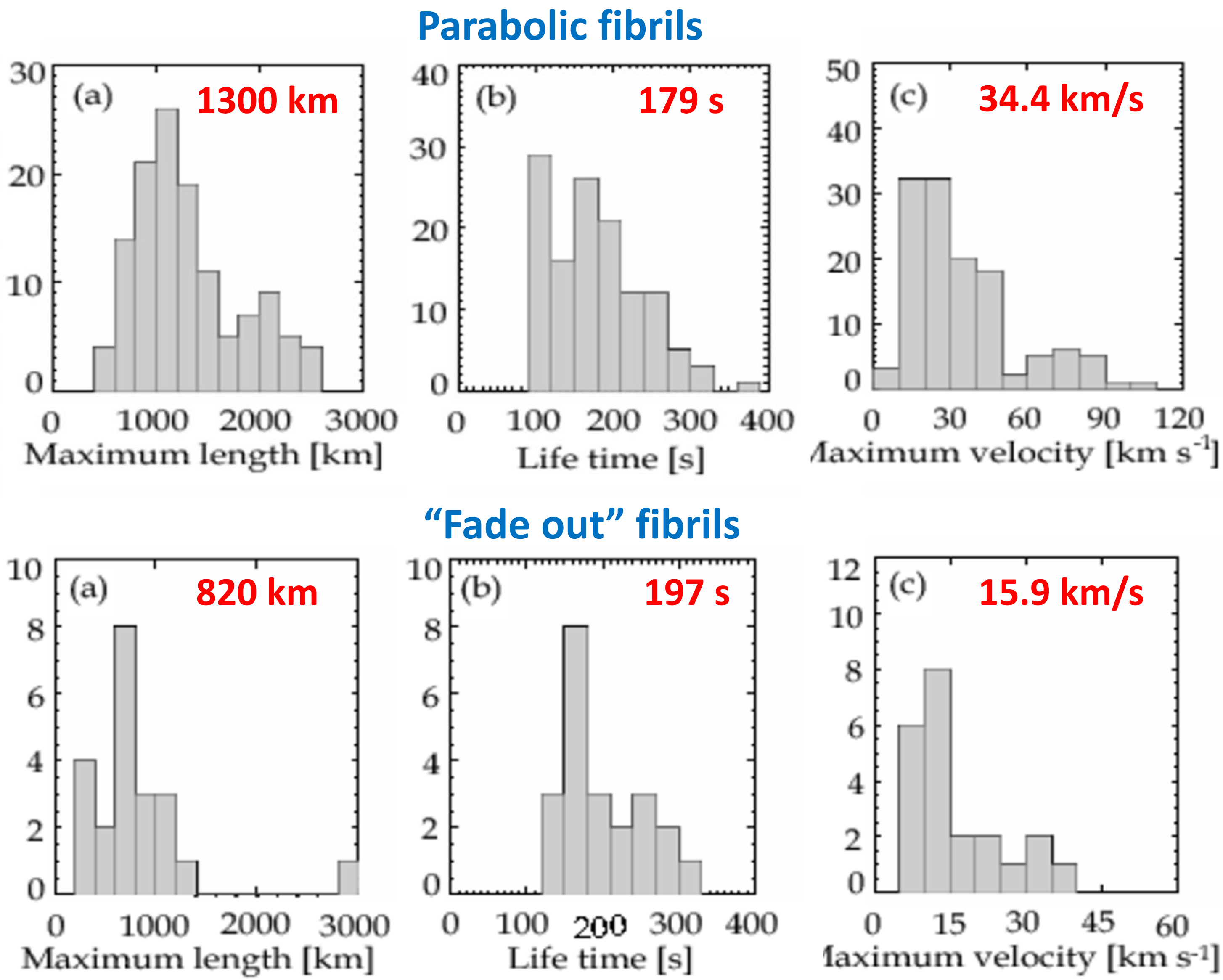

Bi-directional flows

K. Tziotziou[1], G. Tsiropoula[1], and P. Mein[2]

A&A 402, 361–372 (2003)

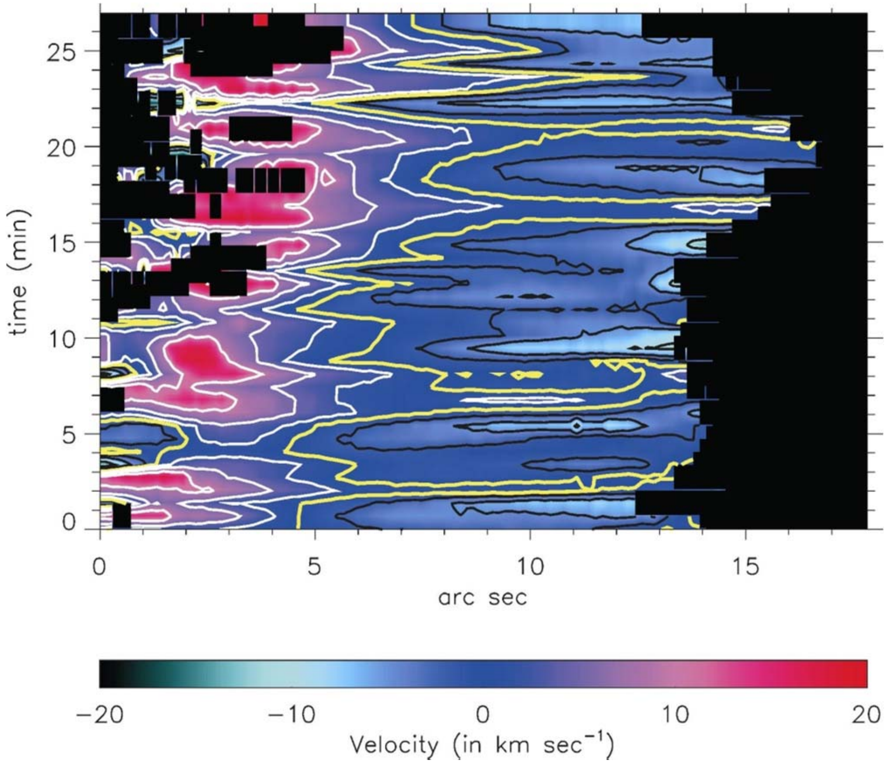

N. Al[1], C. Bendlin[2], J. Hirzberger[3], F. Kneer[2], and J. Trujillo Bueno[4,5]

A&A 418, 1131–1139 (2004)

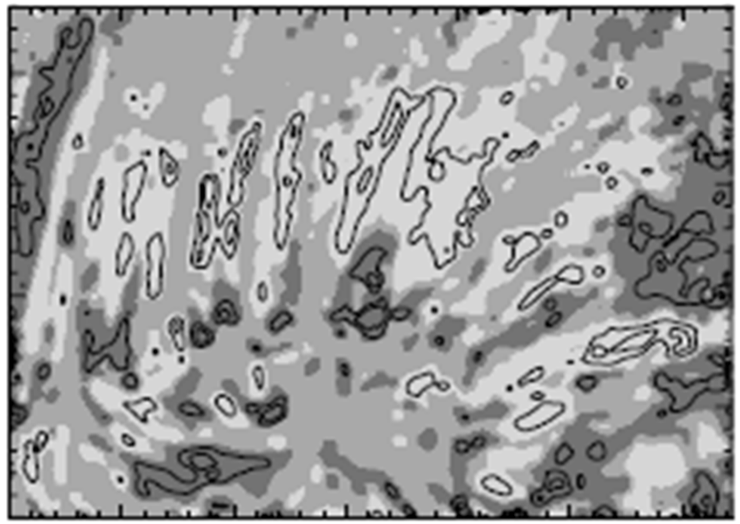

Periodicities

K. Tziotziou[1,*], G. Tsiropoula[1], and P. Mein[2]

A&A 423, 1133–1146 (2004)

Wavelet spectra of an area of mottles

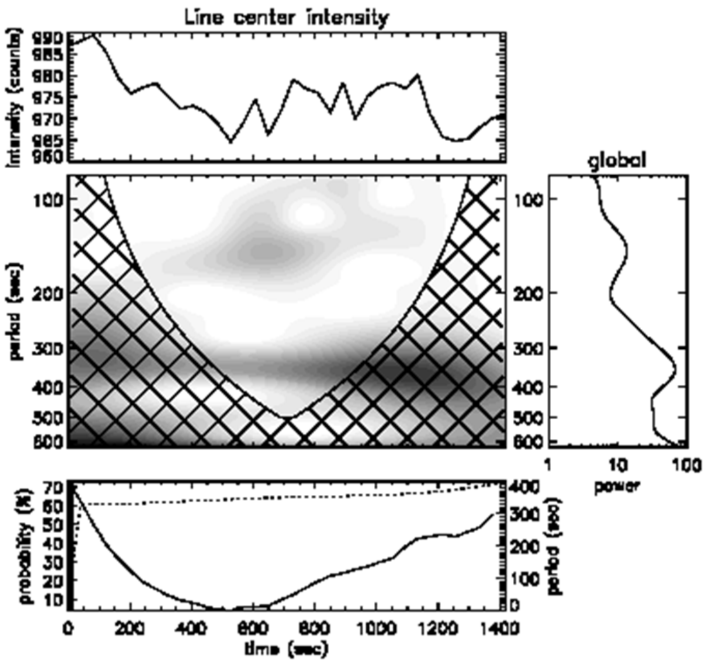

Wavelet spectra along a mottle

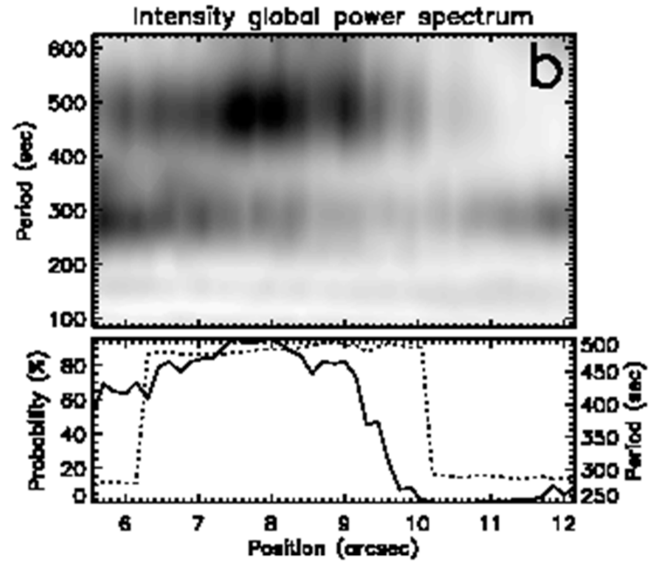

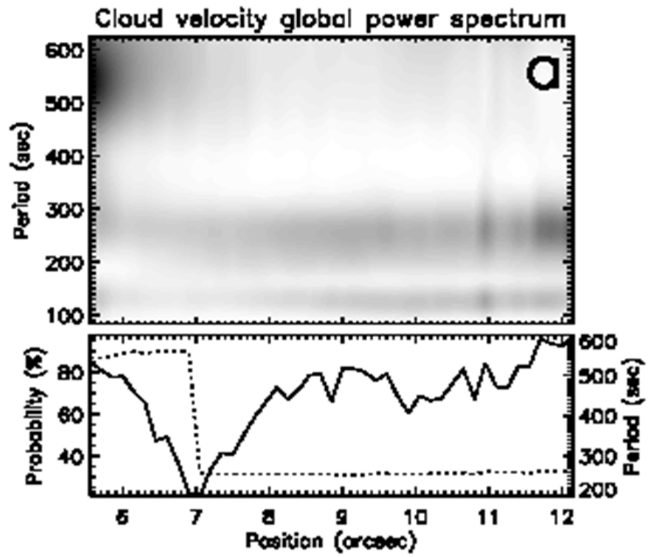

Dominant period ~5min

Does it imply anything about the driver of mottles?

Periodicities

K. Tziotziou[1,*], G. Tsiropoula[1], and P. Mein[2]

A&A 423, 1133–1146 (2004)

Wavelet spectra of an area of mottles

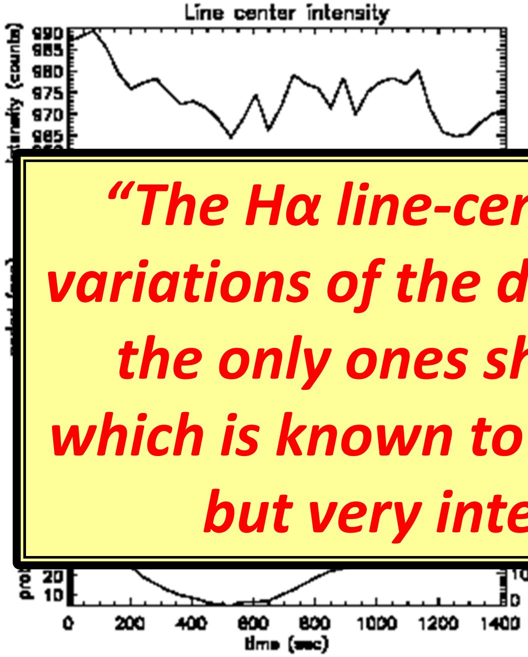

Wavelet
mottle

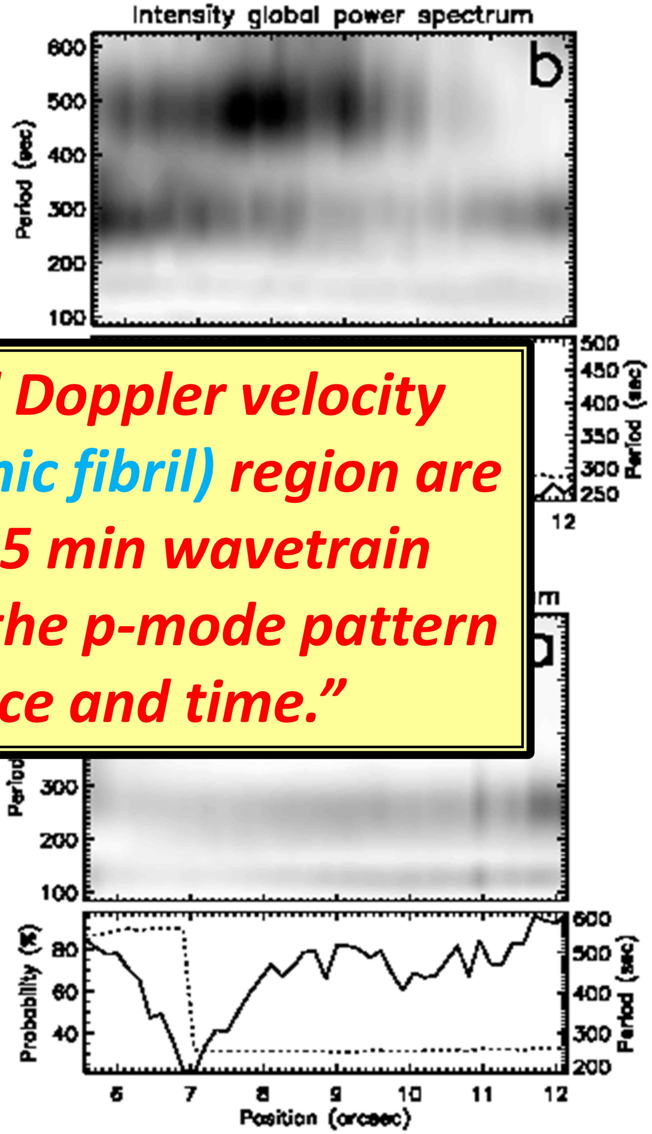

"The Hα line-center intensity and Doppler velocity variations of the dark-grain (dynamic fibril) region are the only ones showing a regular 5 min wavetrain which is known to be produced by the p-mode pattern but very intermittently in space and time."

Dominant period ~5min

Does it imply anything about the driver of mottles?

Periodicities: two populations of mottles?

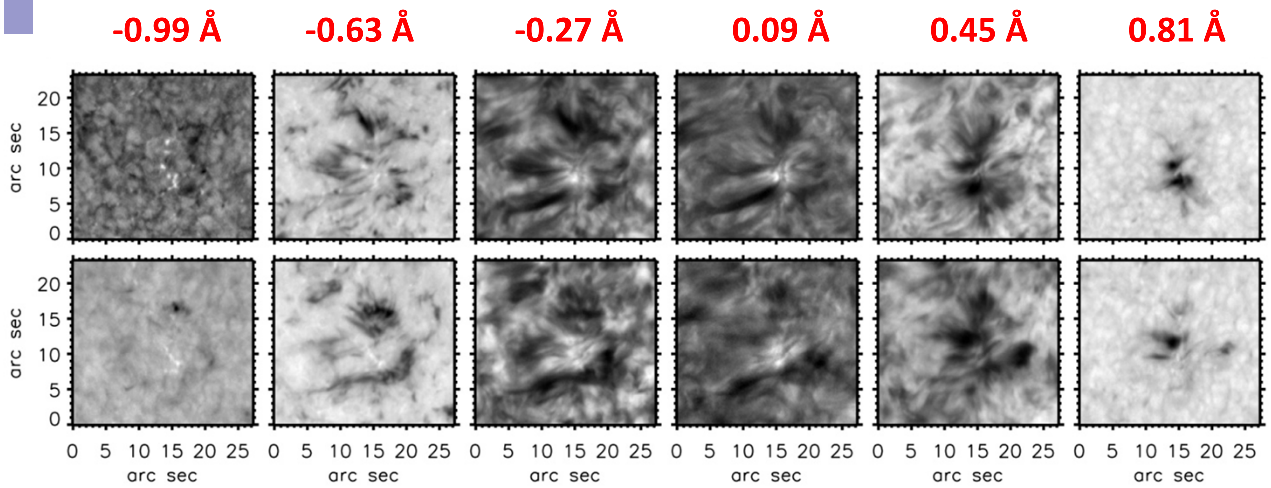

IBIS Hα data at 24 wavelength positions with a constant spectral sampling interval of 90 mÅ and a temporal cadence of 15.4 seconds.

υ < 15 km/s

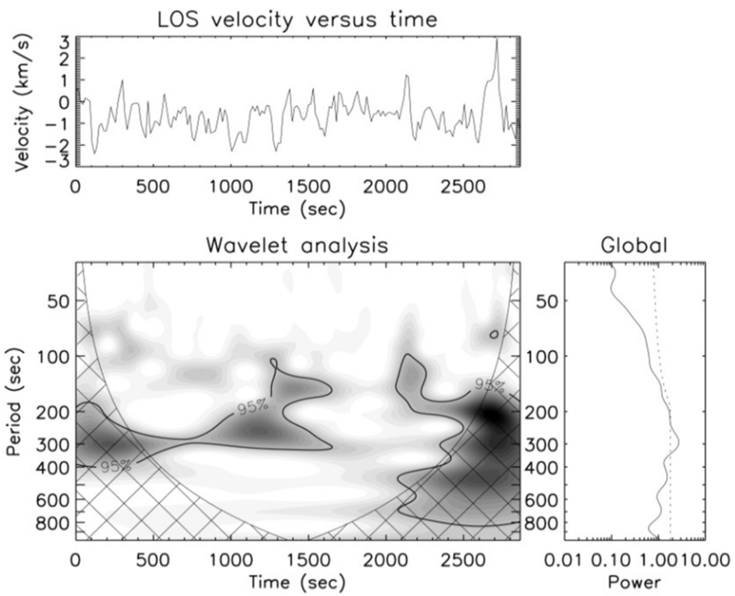

υ > 15 km/s

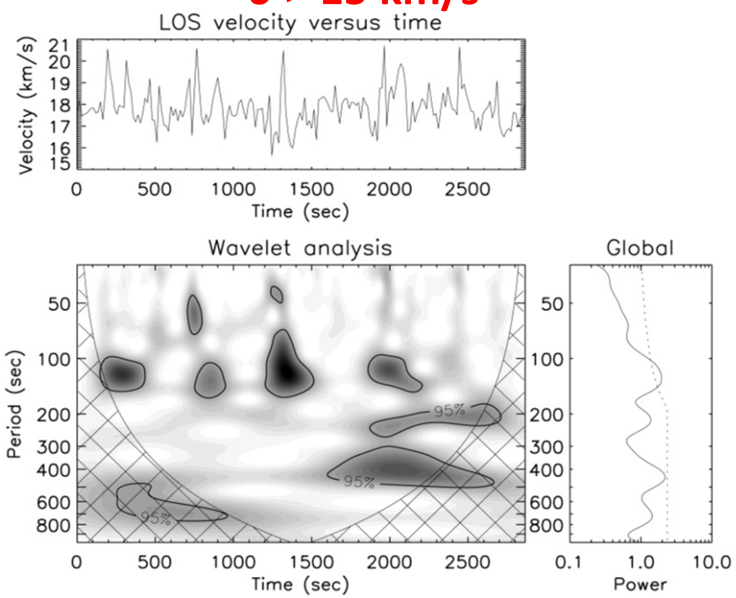

Estimation of magnetic field in spicules

Lopez Ariste & Casini, 2005

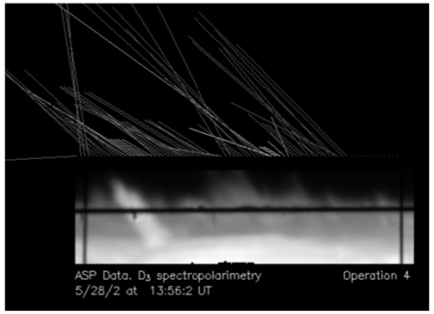

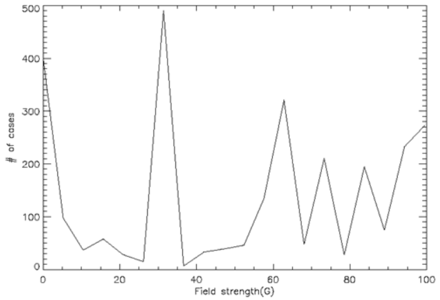

Fig. 7. Distribution of field strengths from inversion of the Stokes parameters plotted in 5 G bins.

Hanle effect He I D3, Sac Peak

- At 3,500 km mostly 10 G
- Some probably up to 40 G?
- 40° from vertical, aligned with spicules?

Trujillo Bueno et al., 2005

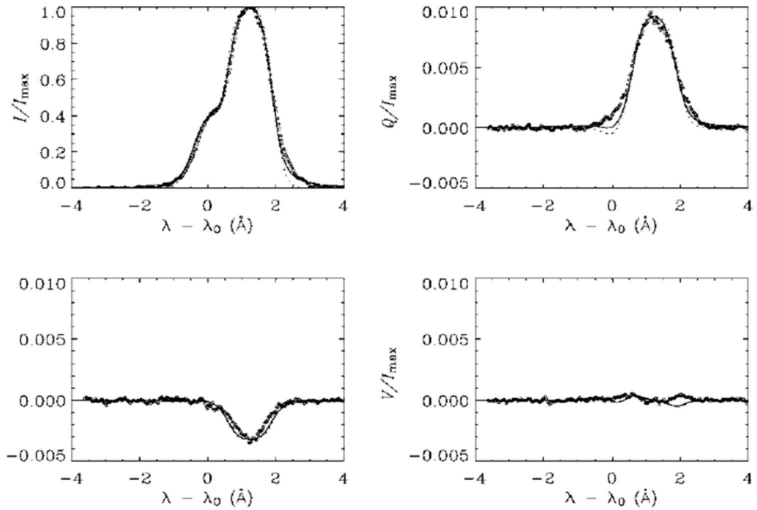

Hanle/Zeeman He I 10830, VTT

- At 2,000 km mostly 10 G
- Some spicules up to 40 G
- Orientation 35° from vertical

Kim et al. 2008
JKAS, 41,173

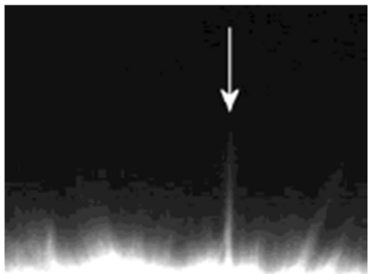

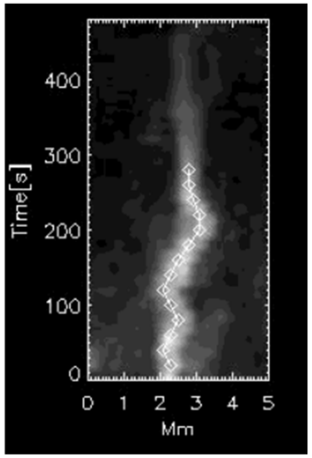

Observed oscillations were interpreted as MHD kink waves propagating through a vertical thin flux tube embedded in a uniform field environment and estimated magnetic field in spicules is about 10-18 G for lower density limit and about 43-76 G for upper density limit

Proposed driving mechanisms for mottles/spicules

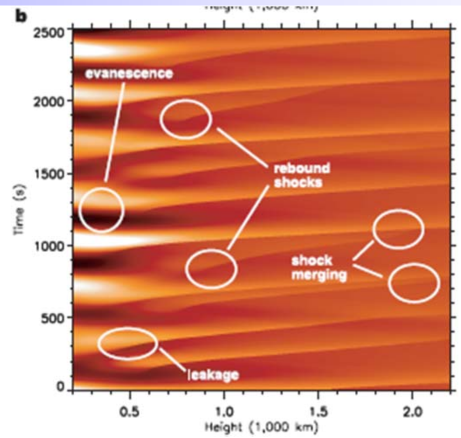

Most possible mechanisms:

- **P-mode leakage in inclined flux tubes**

(Suematsu 1990, De Pontieu et al. 2004)

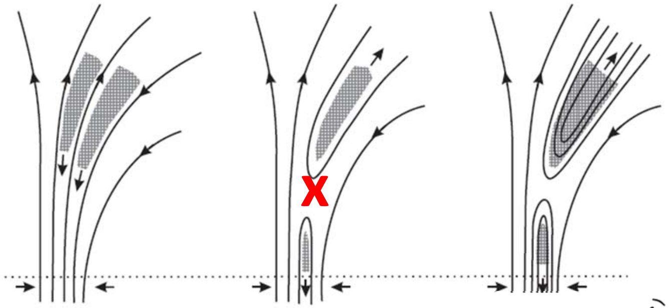

- **Reconnection**

(Pikel'ner 1969, Tziotziou et al. 2003)

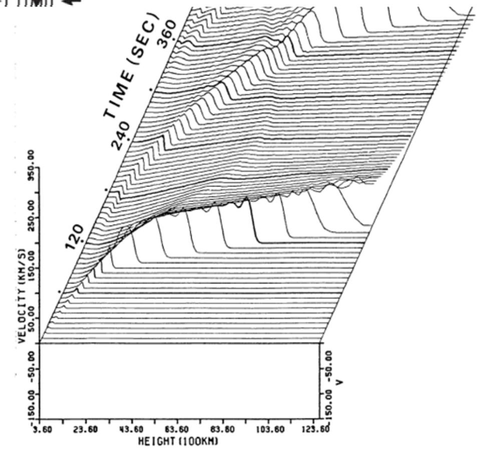

- **Shocks created by pressure enhancements, wave pulses, resonant waves as a result of granular buffeting of flux tubes**

(Roberts 1979, Suematsu 1982, Shibata, 1982, Hollweg 1982)

P-mode leakage

Hypothesis: **Source for spicules probably photospheric?**

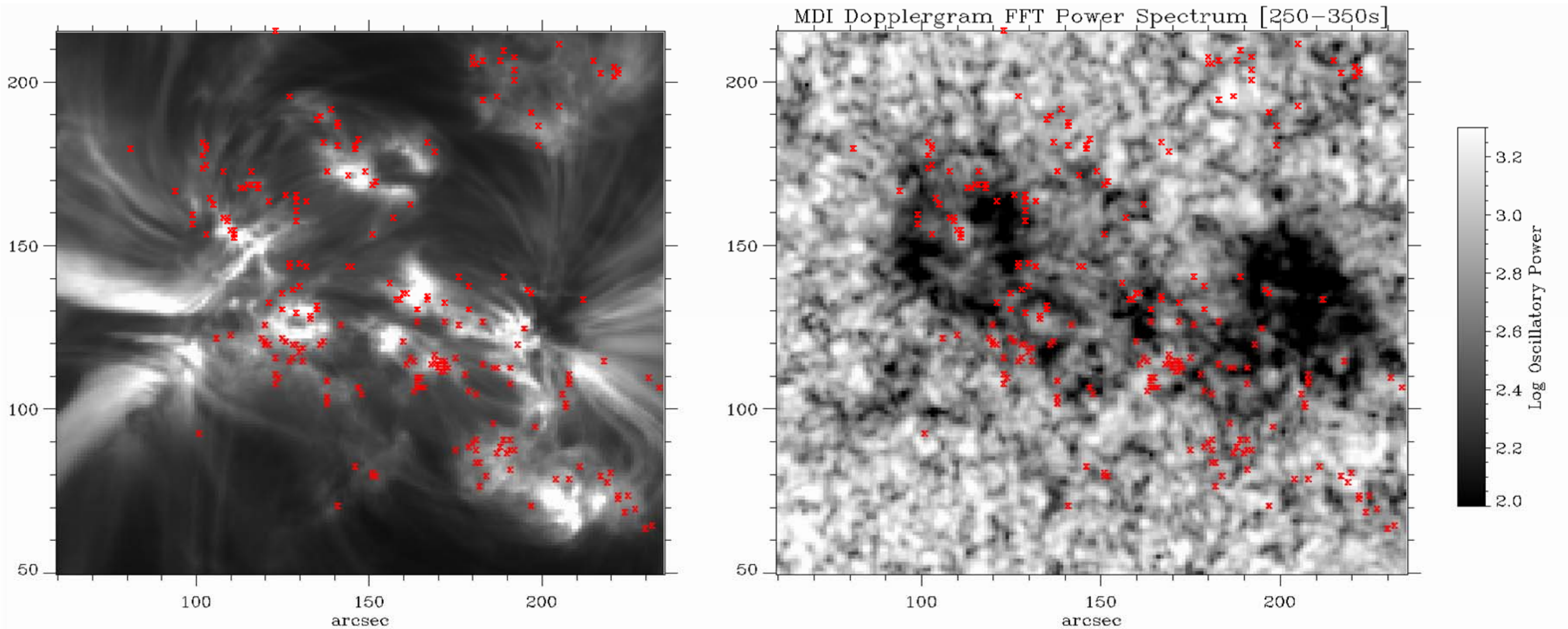

Photosphere dominated by 5-min power (p-modes)

However, p-modes are evanescent…

WHAT DRIVES THEM?

P-mode leakage

- **Big question:** How do evanescent 5-min photospheric oscillations leak into the atmosphere?

- **Answer:** Acoustic cutoff period ~1/cosθ

- Suematsu (1990) proposed the formation of chromospheric fine structure from leaked p-modes in inclined structures

- De Pontieu etal. 2004 performed modeling using MDI driven 1D HD

P-mode leakage

Modeling using MDI driven 1D HD

Vertical Velocity $\theta = 40°$

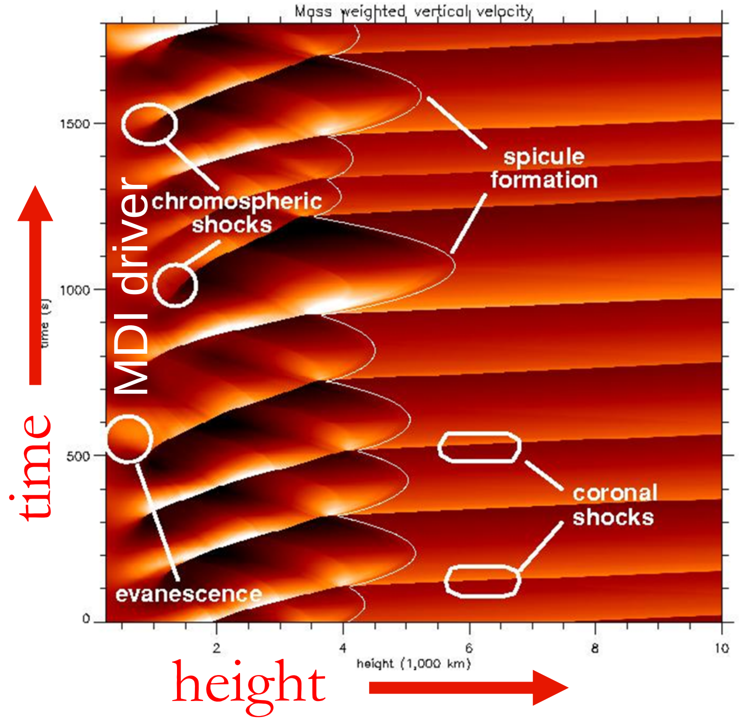

- Active region fibrils
- Periodic spicules from p-mode leakage on inclined or twisted flux tubes
- Most spicules *not periodic*
- 2D or 3D simulations with proper non-LTE radiation treatment necessary…

P-mode leakage

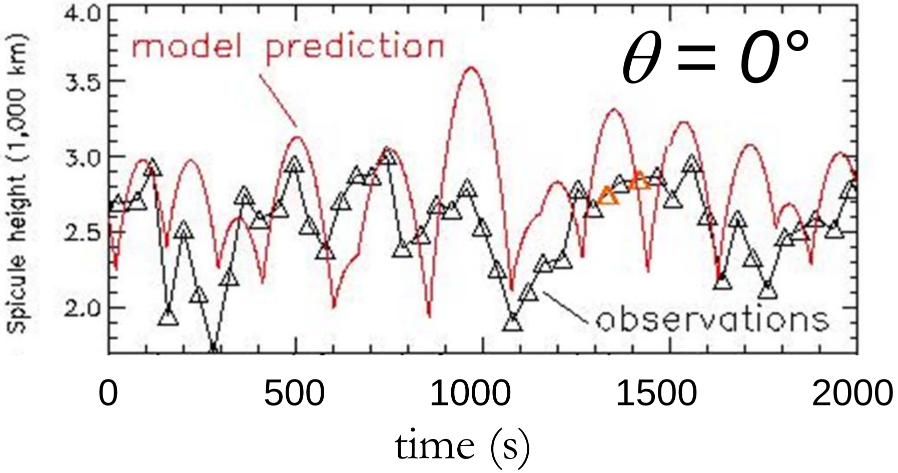

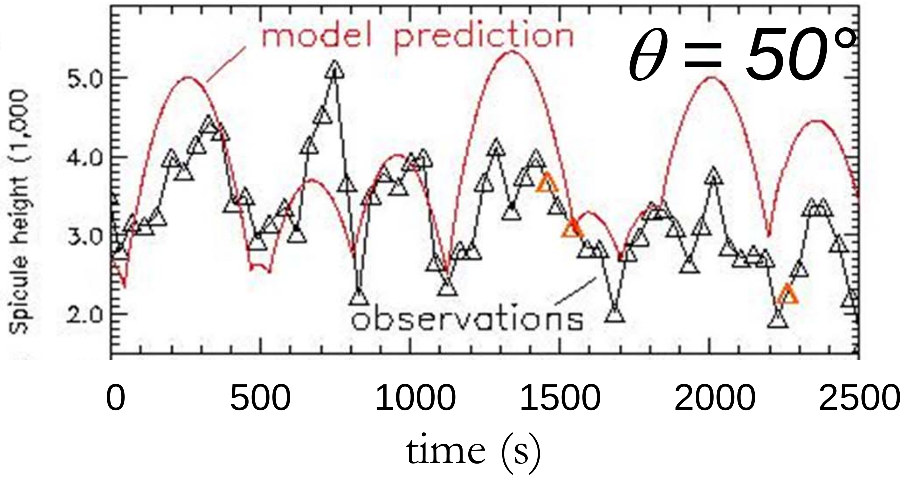

Predicted and observed spicule occurrence agree reasonably well
Mismatch in amplitude due to varying filling factors

<u>However:</u>

- **obtained velocities from simulation are too small**
- **magnetic field boundary values are too high**
- **and most importantly what happens to the magnetic field that cumulates in network boundaries?**

Reconnection

Observational evidence

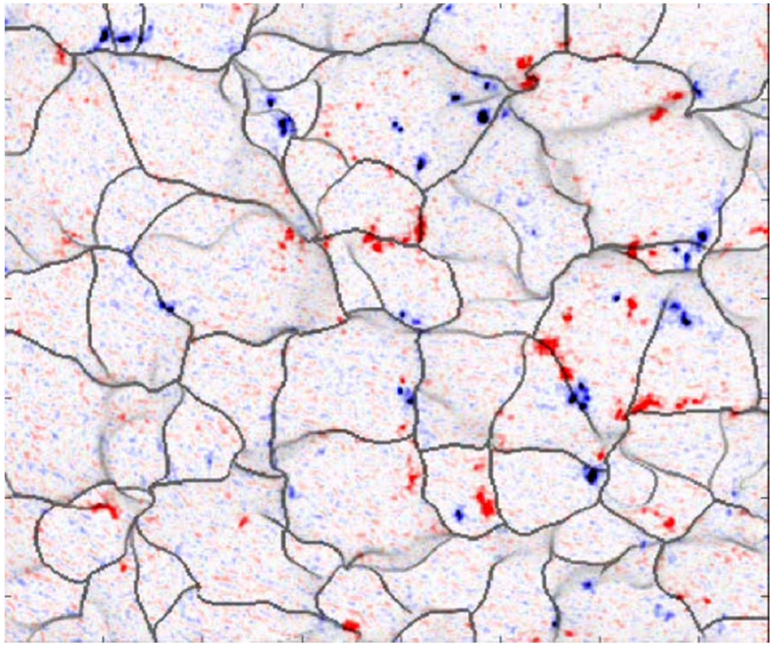

K. Tziotziou[1], G. Tsiropoula[1], and P. Mein[2]

A&A 402, 361–372 (2003)

Bi-directional flows

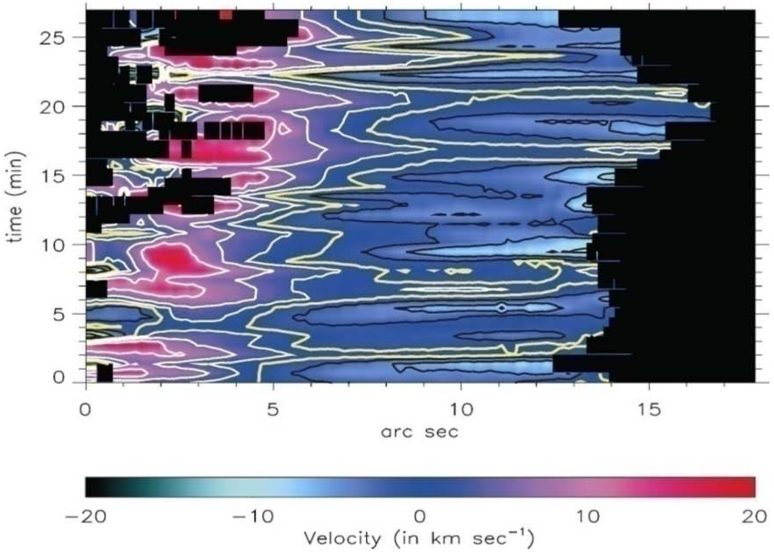

Temperature enhancement

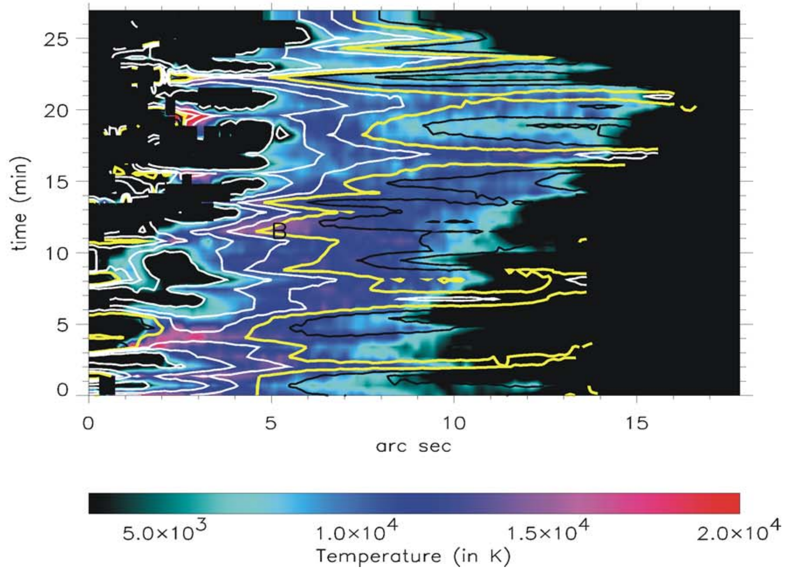

Reconnection

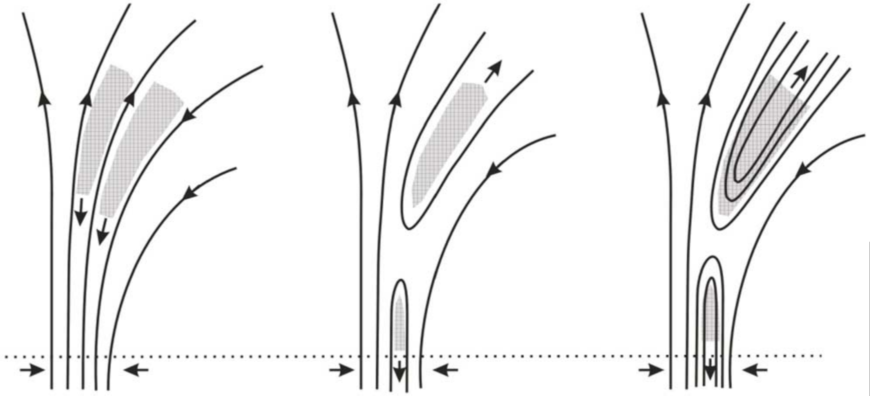

Squeezing of opposite polarity fields

Cooling by radiation of compressed gas and downflow

Reconnection of magnetic fields

Upflows and downflows

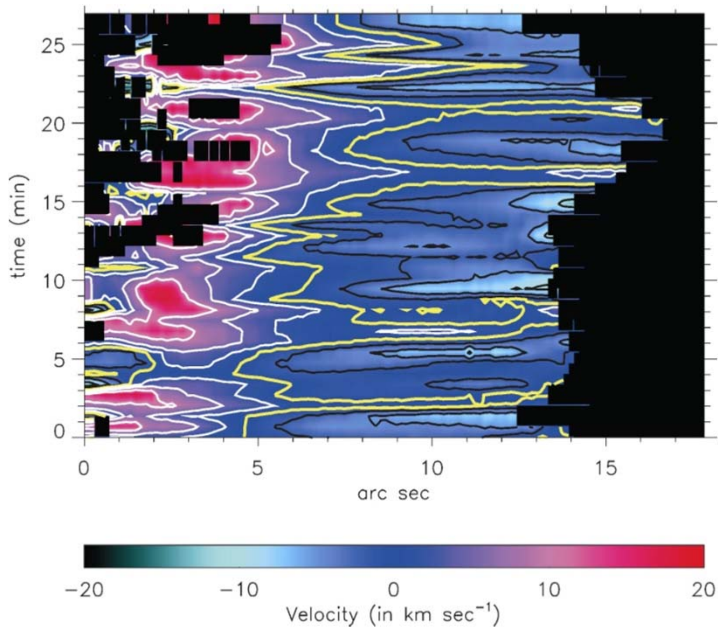

Reconnection explains observed bi-directional behaviour and provides high velocities

Probably need to incorporate both waves and reconnection!

Chromospheric Alfvénic Waves

Example of transverse displacement of a spicule

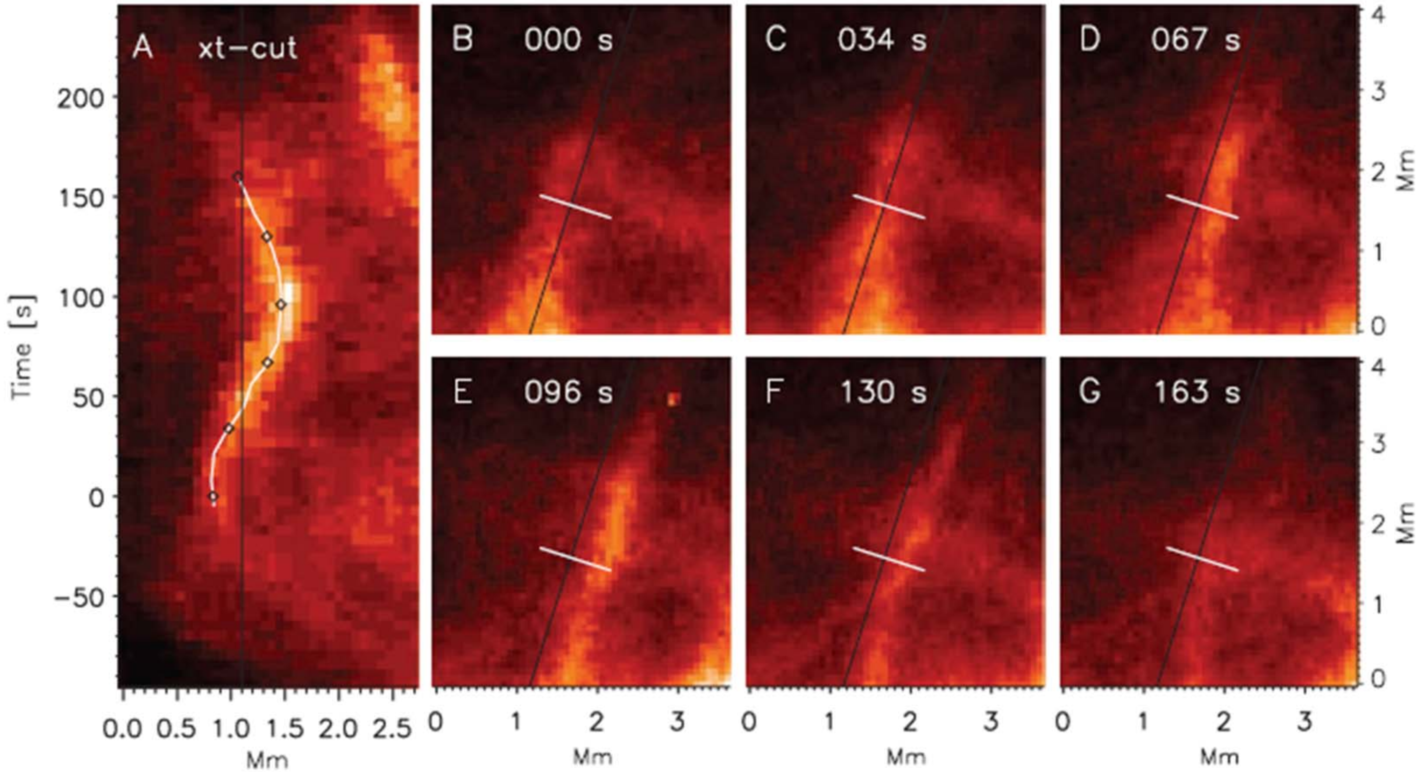

B. De Pontieu, *et al.*
Science **318**, 1574 (2007)

Chromospheric Alfvénic Waves

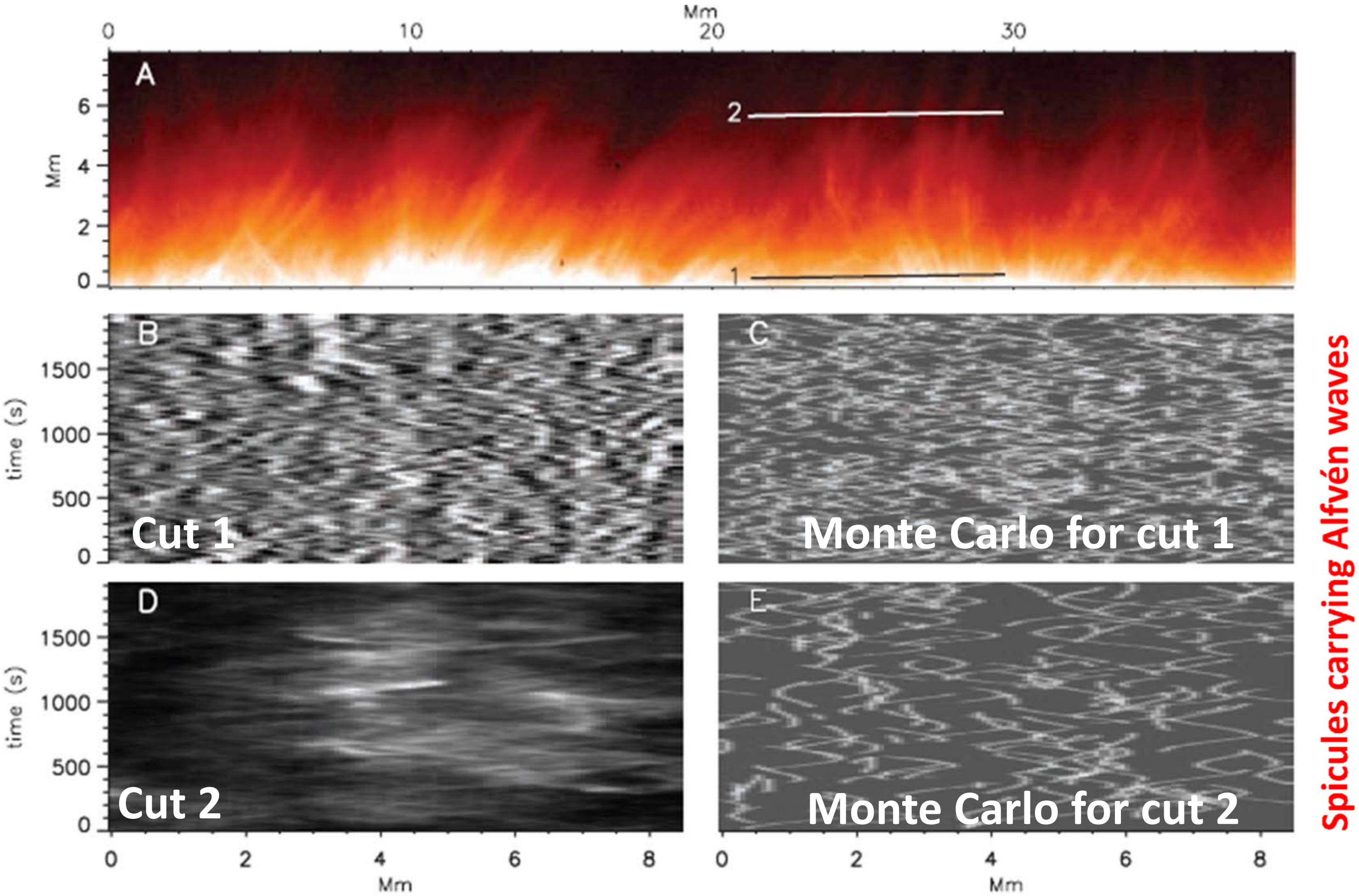

B. De Pontieu, *et al.*
Science **318**, 1574 (2007)

Chromospheric Alfvénic Waves

Space-time cut of the Ca II H

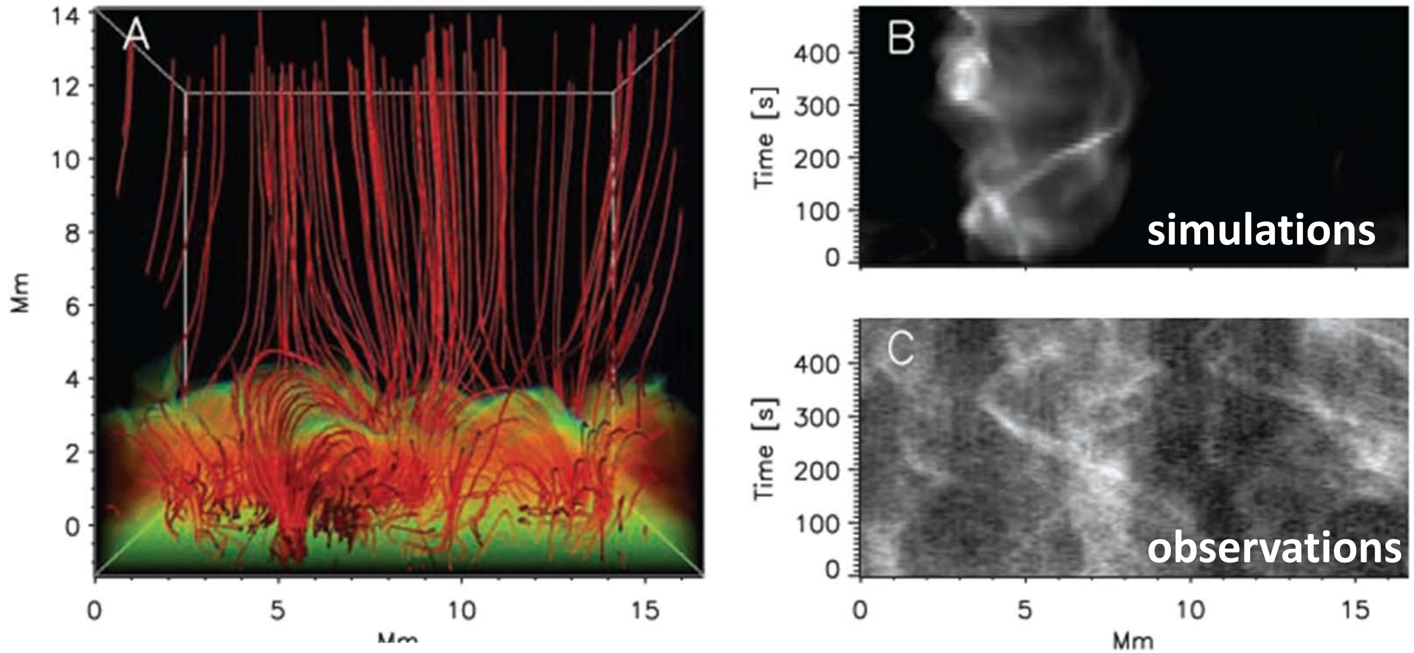

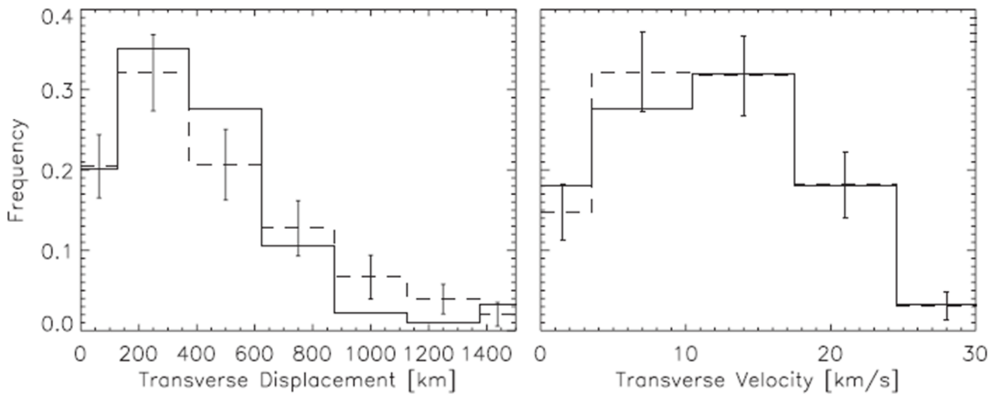

Observed: solid line
Simulated: dashed line

B. De Pontieu, *et al.*
Science **318**, 1574 (2007)

Upward propagating high-frequency Alfvén waves in spicules

Four cases of spicules modulated by high-frequency (≥0.02 Hz) transverse fluctuations, suggesting to be Alfvén waves that propagate upward along the spicules with phase speed ranges from 50 to 150 km s^{-1}. Three of the modulated spicules show clear wave-like shapes with short wavelengths less than 8 Mm.

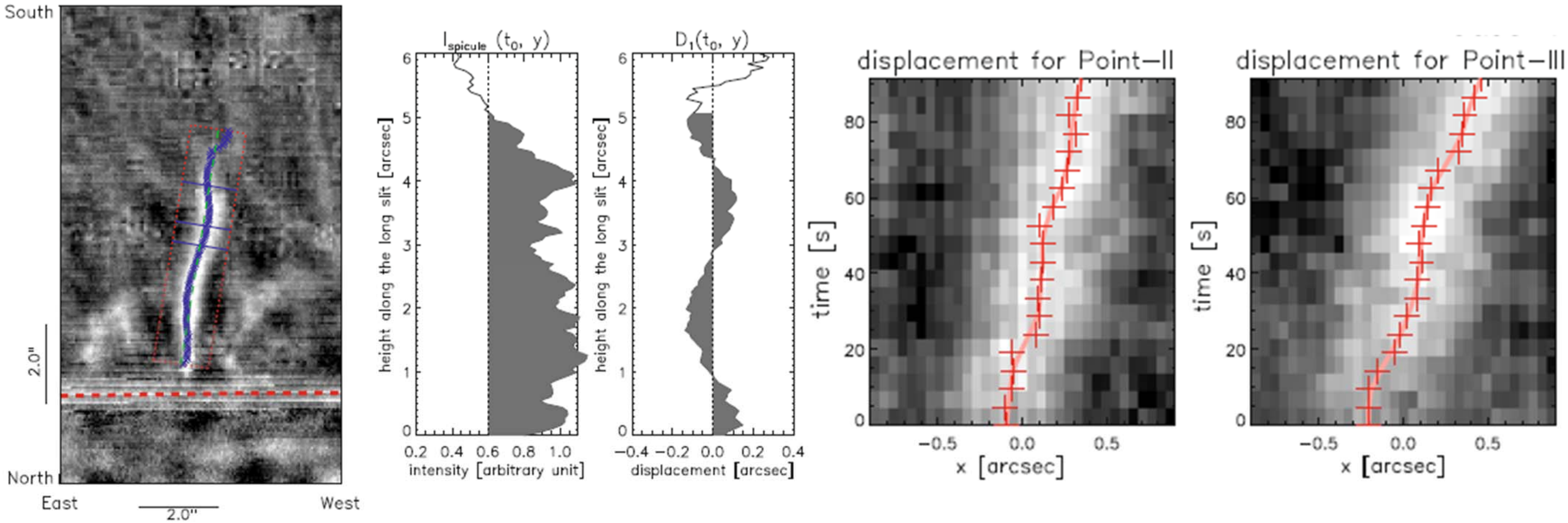

Spicule number	Wave period	Phase speed	Velocity amplitude	Height	Inclination
Spicule-1	48 s	75–150 km s^{-1}	4.7 km s^{-1}	4.4 Mm	10°
Spicule-2	37 s	59–117 km s^{-1}	6.1 km s^{-1}	5.8 Mm	29°
Spicule-3	45 s	73 km s^{-1}	18.1 km s^{-1}	1.5 Mm	43°
Spicule-4	50 s	109–145 km s^{-1}	20.8 km s^{-1}	7.3 Mm	30°

J.-S. He et al. A&A 497, 525–535 (2009)

It's all about magnetic fields!

Kontogiannis et al 2010

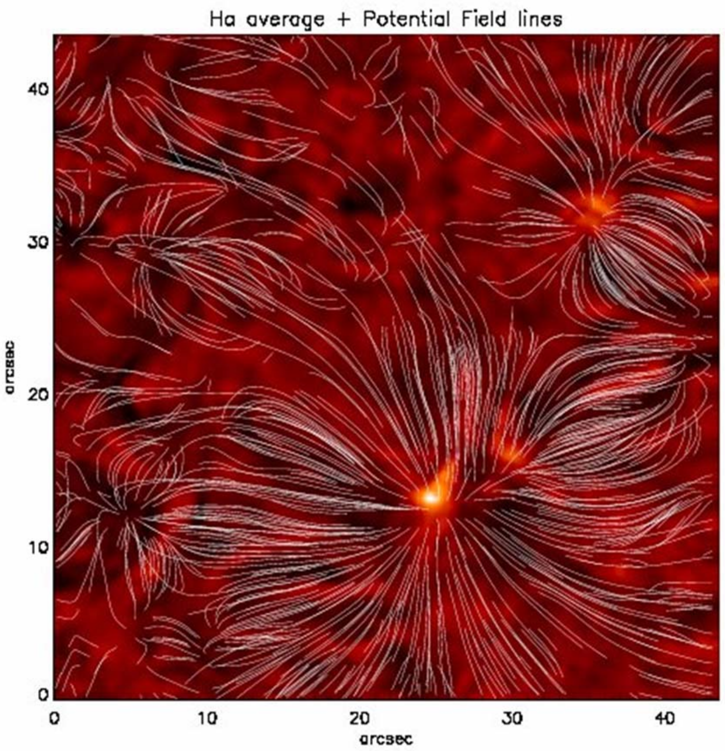

3 min **5 min** **7 min**

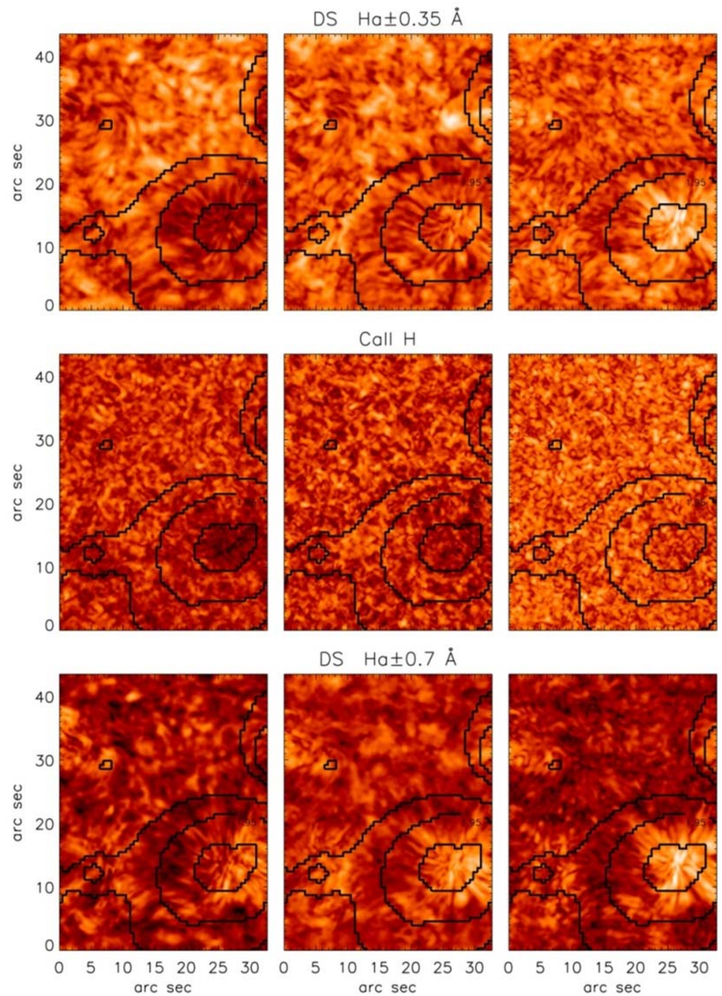

Next talk!

Mass flow to the corona

Assuming that at any moment:

- **only half of the mottles show upward motion only half of the material flows upwards**
- **fraction *f* of the covered solar surface ~ 0.05 (4 10^5 structures)**
- **average mass density ρ (2.2 10^{-13} g cm^{-3})**
- **average axial velocity υ_α (υ_α = 25 km/sec)**

Upward mass flux: $$F_M = \frac{1}{2}(\frac{1}{2} f \rho \upsilon_\alpha) = 7.1\, 10^{-9}\, \mathrm{g\, cm^{-2}\, s^{-1}}$$

Mass outflow from the solar corona: 3 10^{-11} g cm^{-2} s^{-1}

Assuming that the remaining flux $F_f = 0.99 \times F_M$ is falling back as EUV observations indicate and the average mass density ρ_{tr} is 6.7 10^{-15} g cm^{-3} :

$$\upsilon_f = F_f / \rho_{tr} = 11\ \mathrm{km\ sec^{-1}}$$ **Observed velocity!**

G. Tsiropoula and K. Tziotziou A&A 424, 279–288 (2004)

Energy flow to the corona

$$F_{\rm mag} = F_{\rm rad} + F_{\rm cond} + F_{\rm K} + \cancel{F_{\rm W}}$$

$$F_{\rm rad} = \alpha(T) N_e^2 \chi g(T) \frac{L}{2}$$

$$F_{\rm cond} = \kappa \frac{{\rm d}T}{{\rm d}h}$$

$$F_{\rm K} = F_{\rm kin} + F_{\rm h} + F_{\rm g}$$

$$F_{\rm K} = \frac{1}{2}\rho \upsilon^3 + \frac{\gamma p}{(\gamma - 1)}\upsilon \pm \rho g \frac{L cos(\theta)}{2}\upsilon$$

+

Assumptions:
- **duration of outflow-downflow (~150s)**
- **the area of each event**
- **birthrate of events**
- **outflowing and downflowing energy**

$$F_{\rm B} = \frac{B^2}{8\pi}\frac{b}{2}V_{\rm r}$$

Total energy flux: 1.2 10^5 ergs cm^{-2} s^{-1}

B=11 G

Hanle effect gives 10 G
(Trujillo Bueno etal., ApJ, 2005)

½ of this energy is available for heating of corona

~20% of needed energy flux (3 10^5 ergs cm^{-2} s^{-1})

G. Tsiropoula and K. Tziotziou A&A 424, 279–288 (2004)

Energy flow to the corona

Magnetic energy flux in units of 10^5 erg cm^{-2} s^{-1}

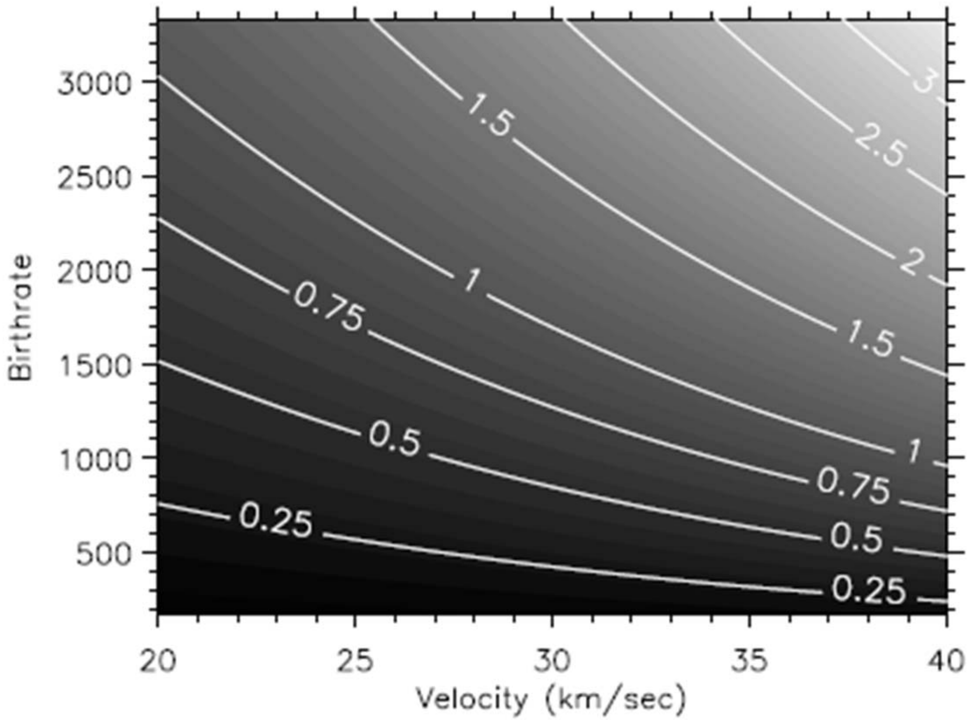

G. Tsiropoula and K. Tziotziou A&A 424, 279–288 (2004)

Energy flow to the corona

MOORE ET AL.

THE ASTROPHYSICAL JOURNAL LETTERS, 731:L18 (5pp), 2011 April 10

Non-thermal Energy Fluxes

Type of Energy Flux and Its Carrier and/or Generator	Symbol	Formula	Estimated Value (erg cm^{-2} s^{-1})
Magnetic-energy flux of EBs	F_{mag}	$F_{mag} \sim (8\pi)^{-1} f_{EB} (B_{EB})^2 D_{EB} (\tau_{EB})^{-1}$	$\sim 1 \times 10^7$
Energy flux of Alfvén waves generated by EBs	F_A	$F_A \sim (4\pi)^{-1/2} f_{gen} f_{EB} (\rho_{II})^{1/2} (v_{lat})^2 B$	$\sim 3 \times 10^5$
Kinetic-energy flux of Type-II spicules generated by EBs	F_{kin}	$F_{kin} \sim (1/2) f_{II} \rho_{II} (v_{II})^3$	$\sim 3 \times 10^5$
Potential-energy flux of Type-II spicules generated by EBs	F_{pot}	$F_{pot} \sim g f_{II} L_{II} \rho_{II} v_{II}$	$\sim 8 \times 10^4$
Work–energy flux of Type-II spicules generated by EBs	F_{work}	$F_{work} \sim f_{II} p_{II} v_{II}$	$\sim 1 \times 10^4$
Total mechanical-energy flux of Alfvén waves and Type-II spicules generated by EBs	F_{mech}	$F_{mech} = F_A + F_{kin} + F_{pot} + F_{work}$	$\sim 7 \times 10^5$

"The value of ~7×10^5 erg cm^{-2} s^{-1} for F$_{mech}$ is comparable to the ~5×10^5 erg cm^{-2} s^{-1} needed to power the coronal heating and solar wind in quiet regions and coronal holes"

Roots of coronal heating in the chromosphere?

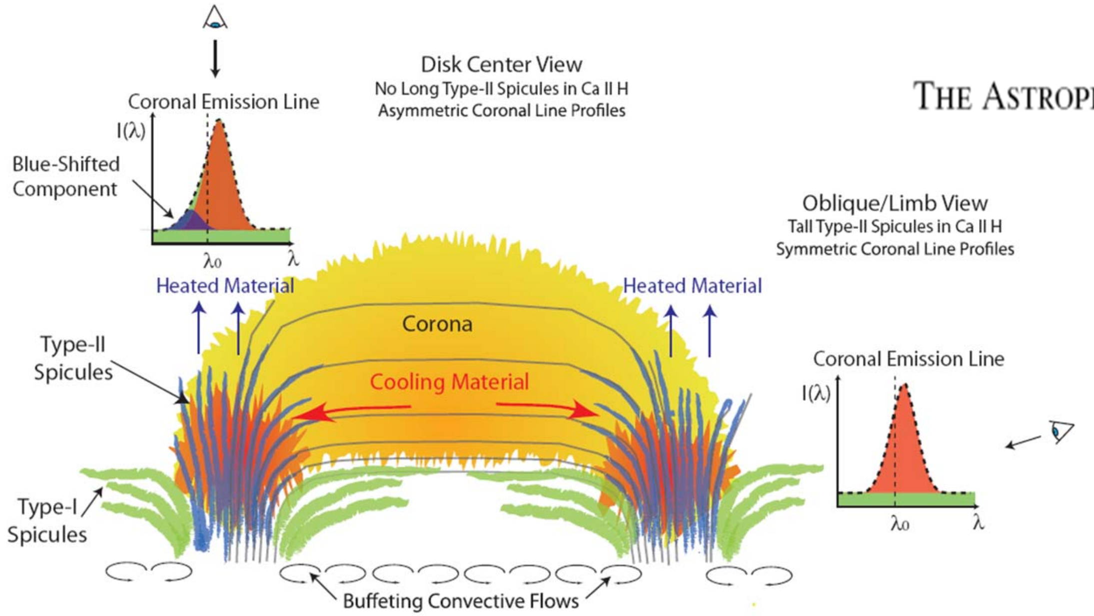

DE PONTIEU ET AL.

THE ASTROPHYSICAL JOURNAL, 701:L1–L6, 2009 August 10

Spectral line profiles of the coronal Fe XIV line show a deviation from a Gaussian indicative of hot plasma flowing upward at high speeds

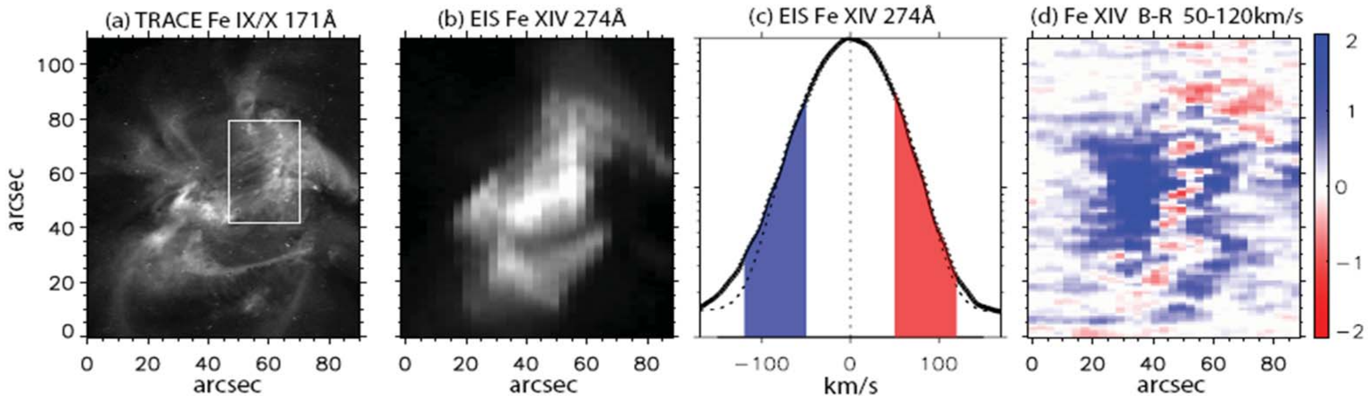

Roots of coronal heating in the chromosphere?

DE PONTIEU ET AL.
THE ASTROPHYSICAL JOURNAL, 701:L1–L6, 2009 August 10

Histogram of upward velocities in chromospheric type II spicules (black line) as derived from Ca II H timeseries at the limb and upflow velocities derived from subtracting a Gaussian fit from the profile of Fe XIV 264 Å (blue) and Fe XIV 274 Å (green)

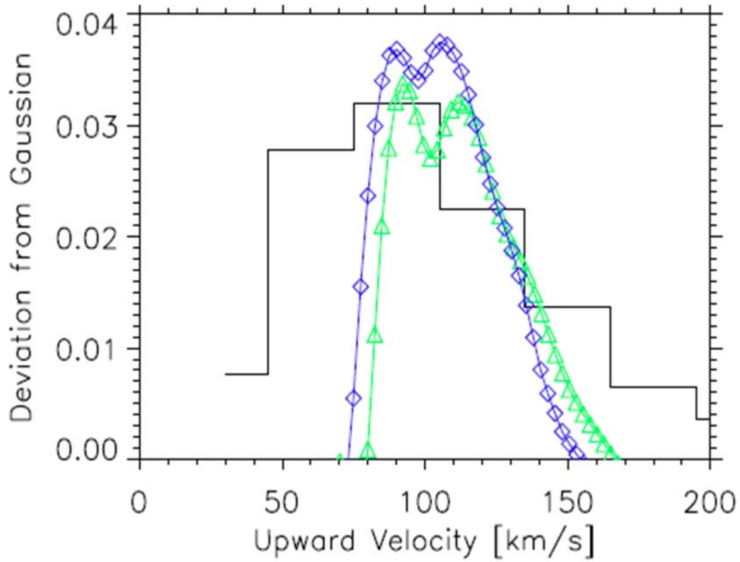

B–R asymmetry maps show strong enhancement of the blue wing emission in the magnetic network (solid black contours)

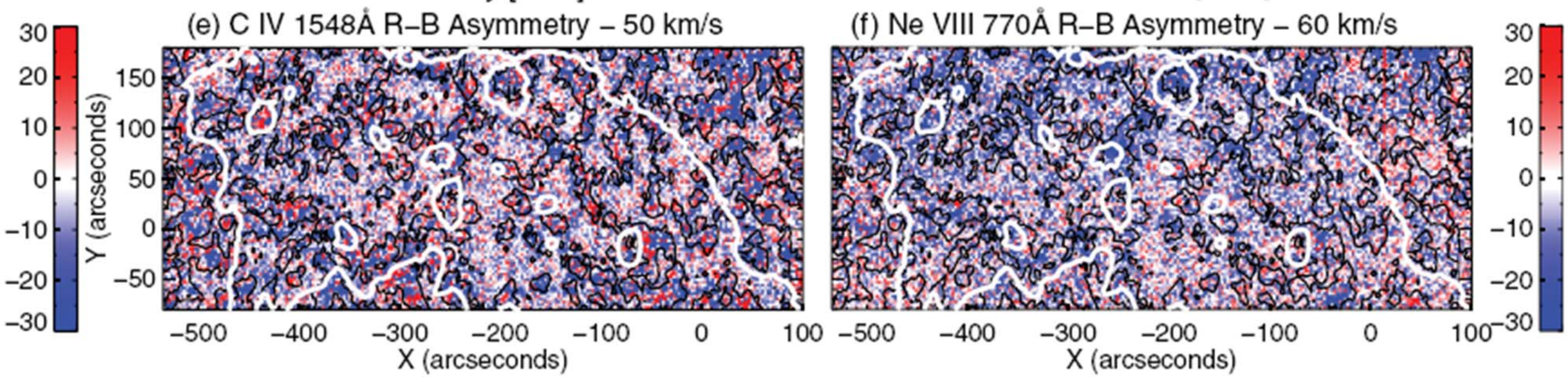

Non-linear propagation of Alfvén waves

MHD simulations of Alfven wave propagation along an open flux tube in the solar atmosphere, generated by photospheric granular motion

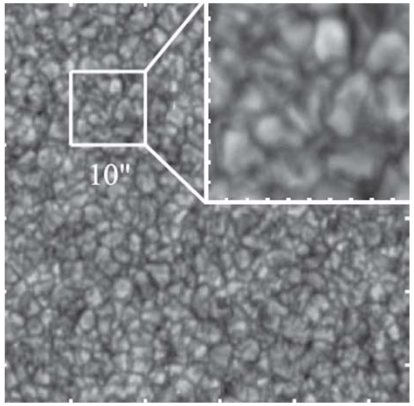

+

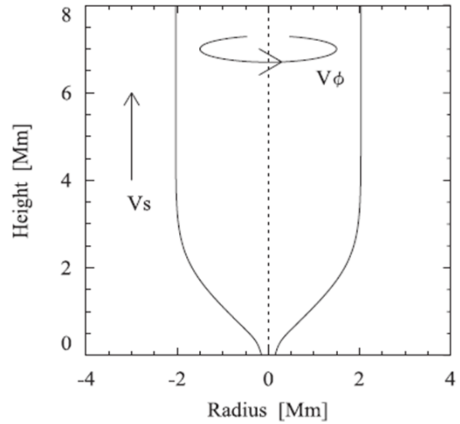

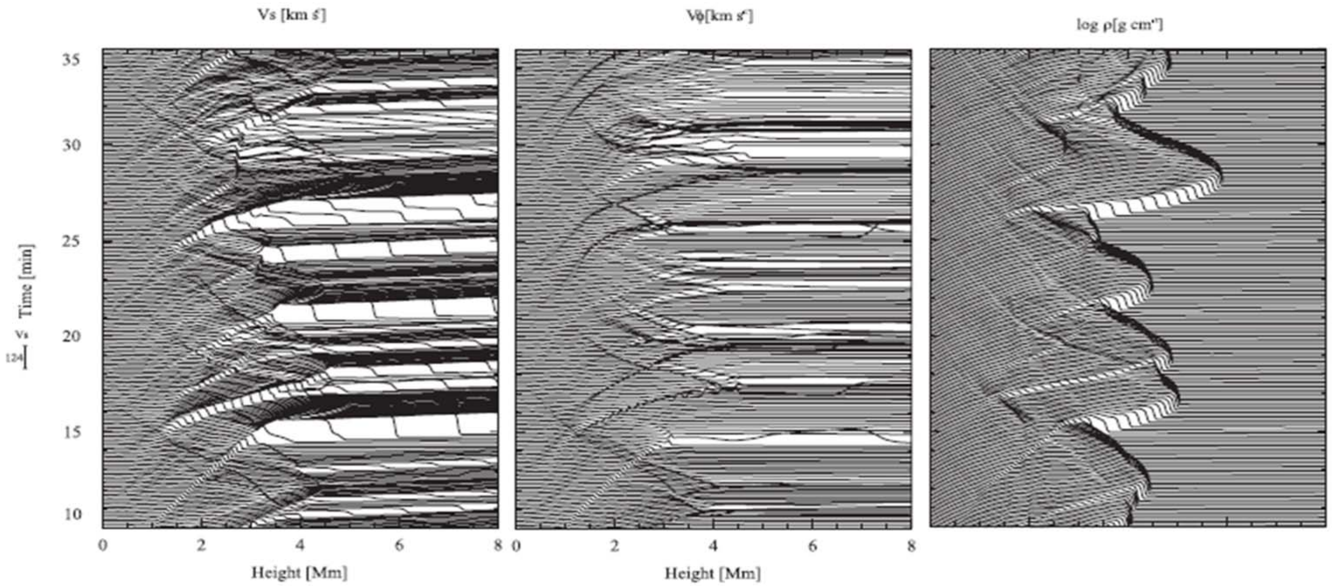

MATSUMOTO & SHIBATA THE ASTROPHYSICAL JOURNAL, 710:1857–1867, 2010 February 20

Non-linear propagation of Alfvén waves

The region between the photosphere and the transition region becomes an Alfven wave resonant cavity. There are at least three resonant frequencies, 1, 3, and 5 mHz. If this cavity exists the resonant periods are expected to be observed as spicule motion or coronal transverse velocity.

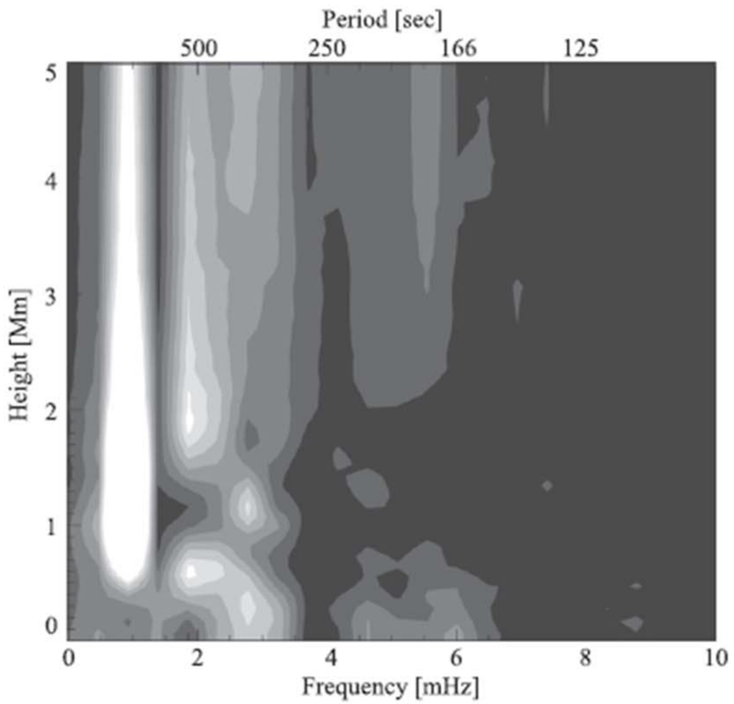

Total energy flux measured at the corona. The amplitude of each wave period is fixed to 1 km/s

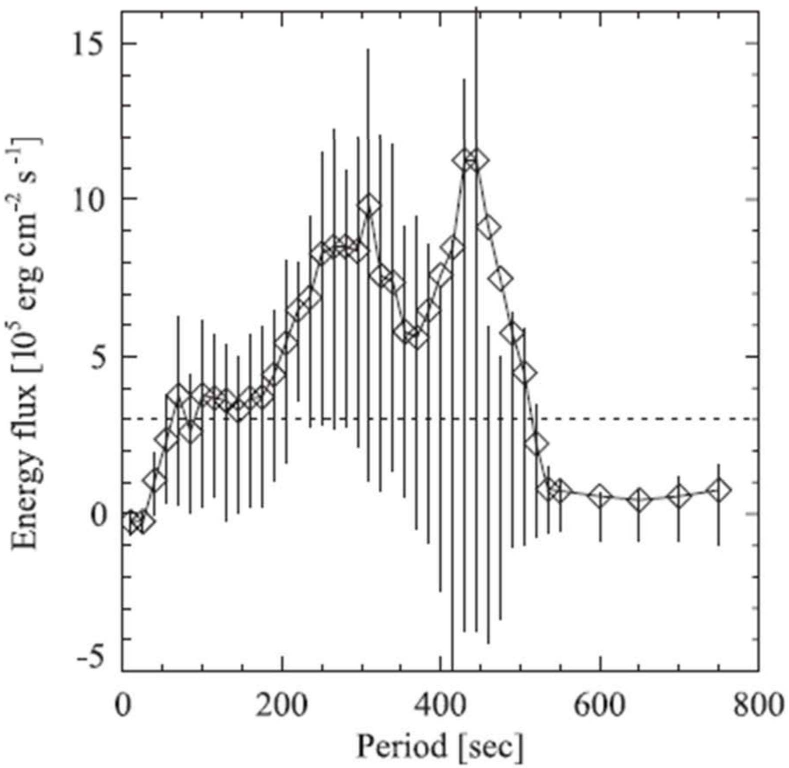

MATSUMOTO & SHIBATA THE ASTROPHYSICAL JOURNAL, 710:1857–1867, 2010 February 20

Formal solutions of the transfer equation

Use given (ad-hoc) source functions, including a stratified chromosphere from which spicules emanate with model parameters compatible with earlier studies of spicules. Spicules are treated statistically, both in their spatial distributions and thermodynamic properties.

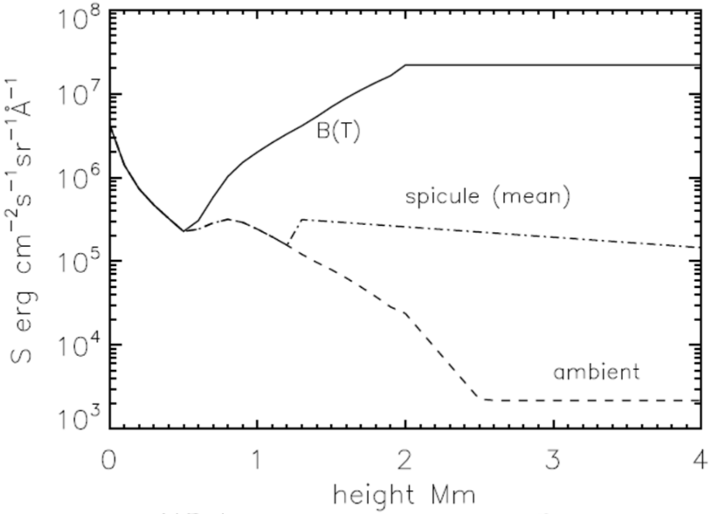

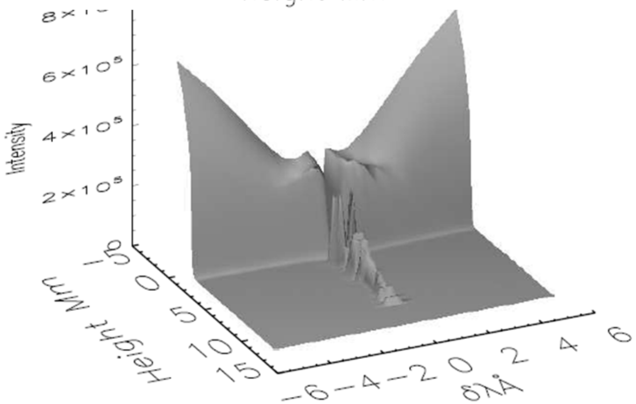

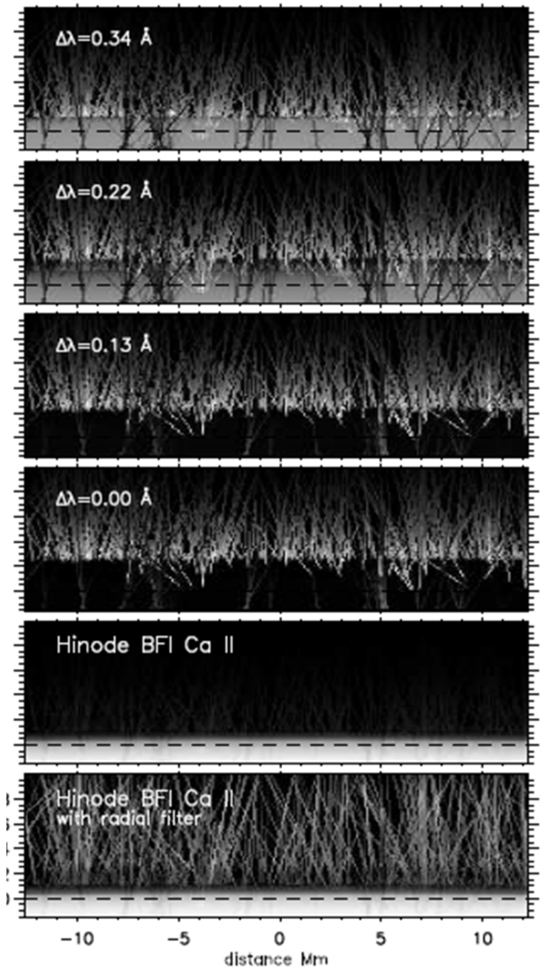

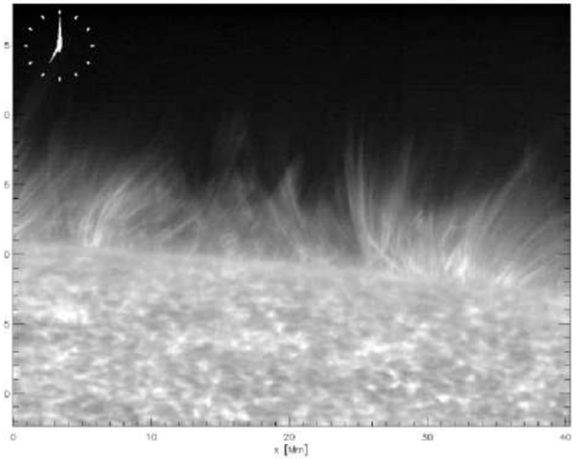

The visibility of Ca II spicules down to the limb in Hinode data seems to require that spicule emission is Doppler shifted relative to the stratified atmosphere, either by supersonic turbulent or organized spicular motion.

Judge & Carlsson, 2010

Dynamic fibrils driven by magnetoacoustic shocks

Dynamic fibrils (type I) driven by leakage of p-modes in inclined magnetic fields

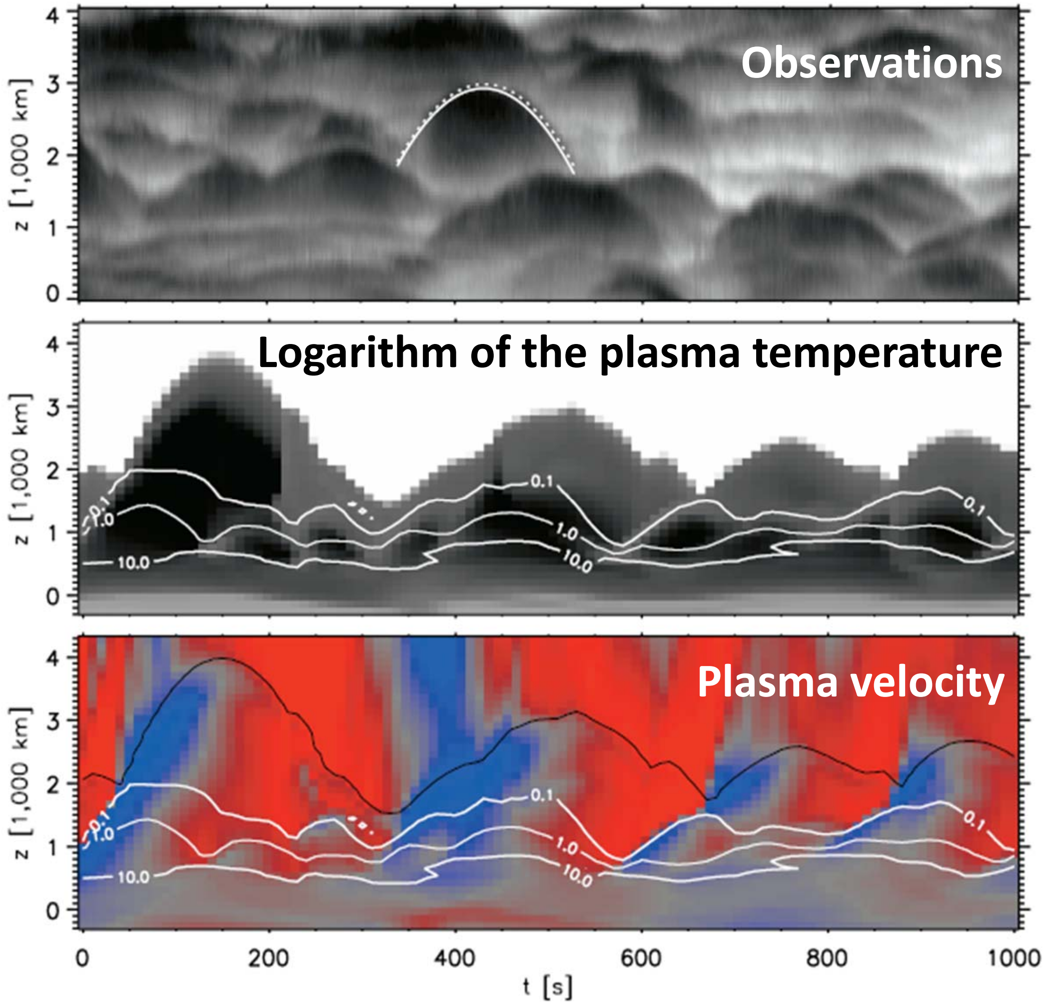

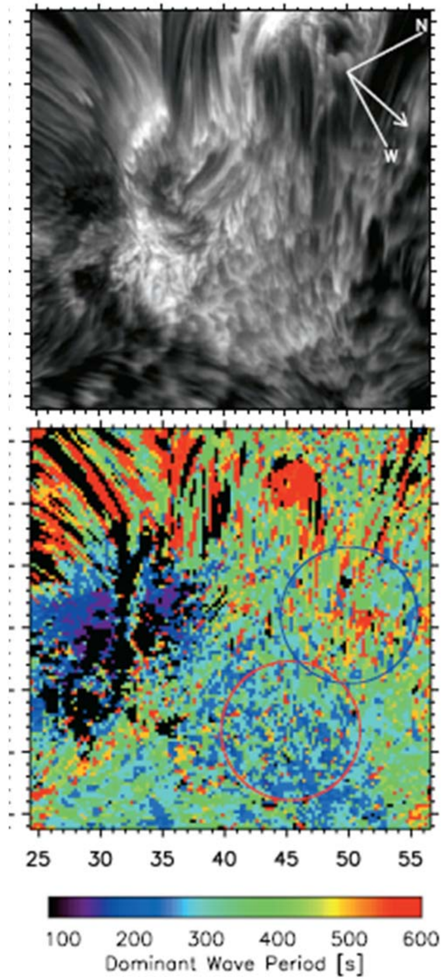

HANSTEEN ET AL. THE ASTROPHYSICAL JOURNAL, 647: L73–L76, 2006 August 10

3-D simulations of Type I and Type II spicules

Magnetic field geometry and connection to the photosphere of a spicule driven by a collapsing granule

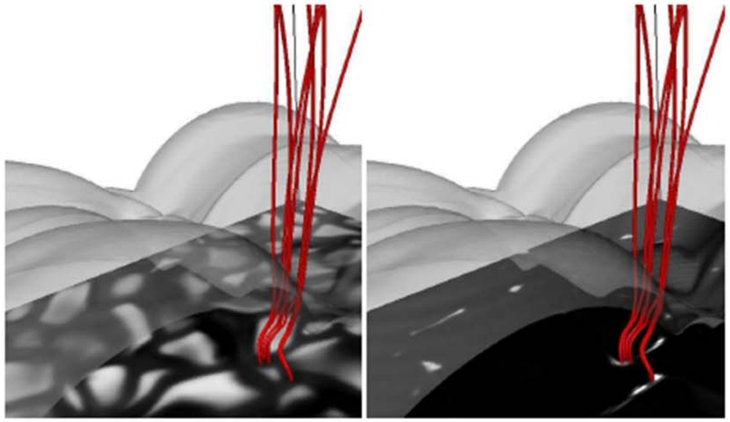

Collapsing granule | **Photospheric energy release** | **Chromospheric energy release**

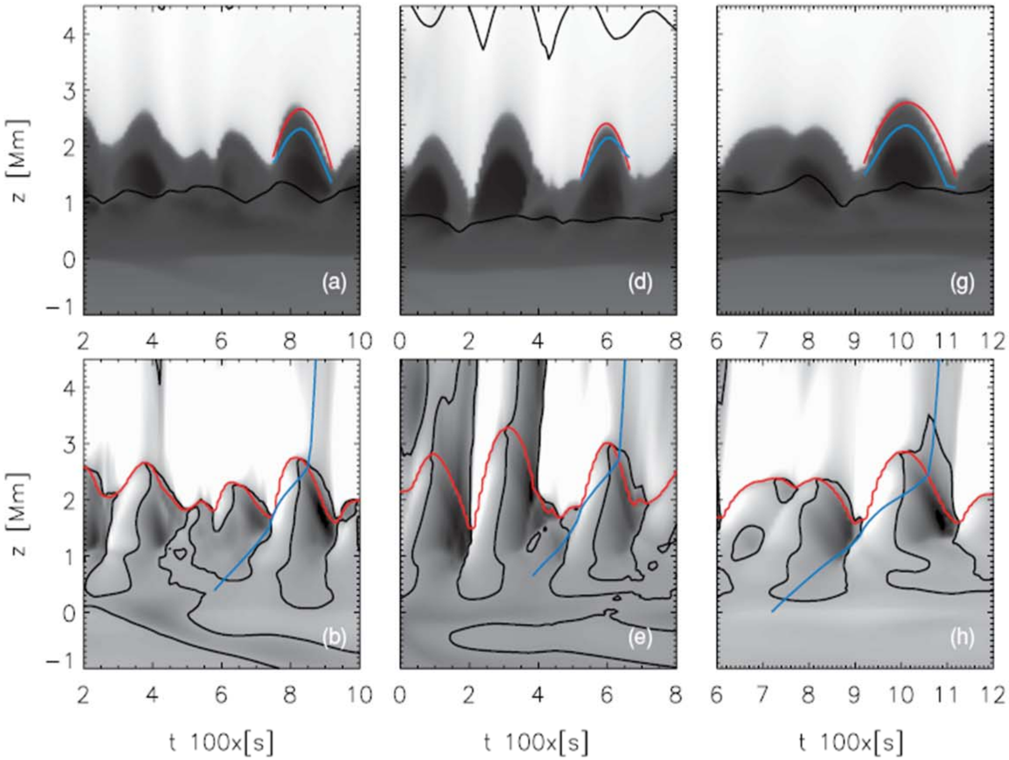

Juan Martínez-Sykora et al, 2009, ApJ 701, 1569

Wave-induced magnetic reconnection

Piston with 300 s period and 1.1 km s^{-1} amplitude (typical of solar granulation)

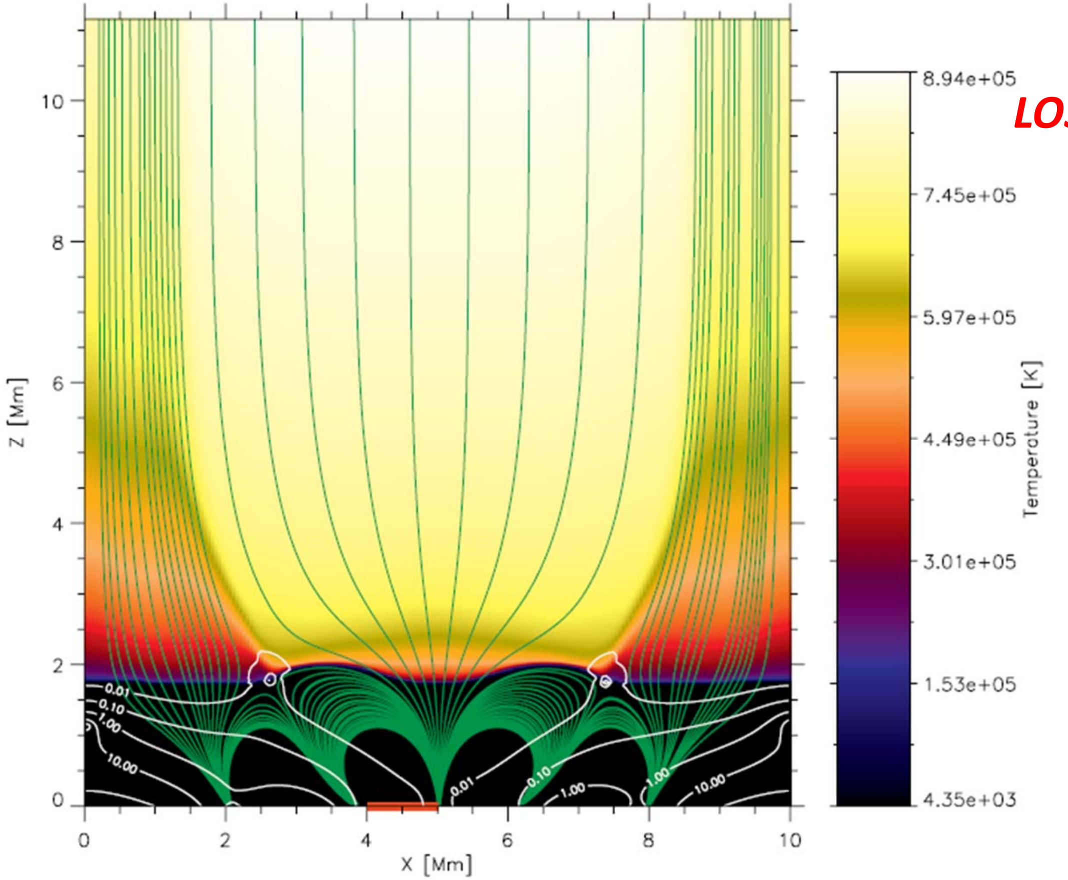

Hinode driver
LOS velocities across slice in network

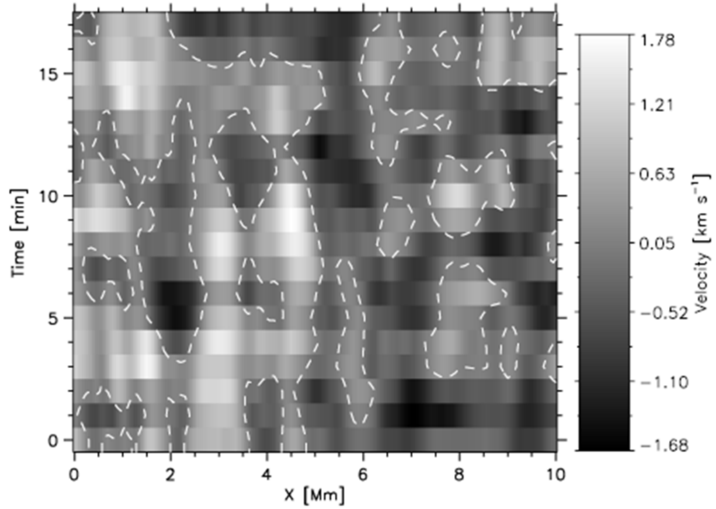

HEGGLAND, DE PONTIEU, & HANSTEEN
THE ASTROPHYSICAL JOURNAL, 702:1–18, 2009 September 1

Wave-induced magnetic reconnection

Transition region null points and piston driver

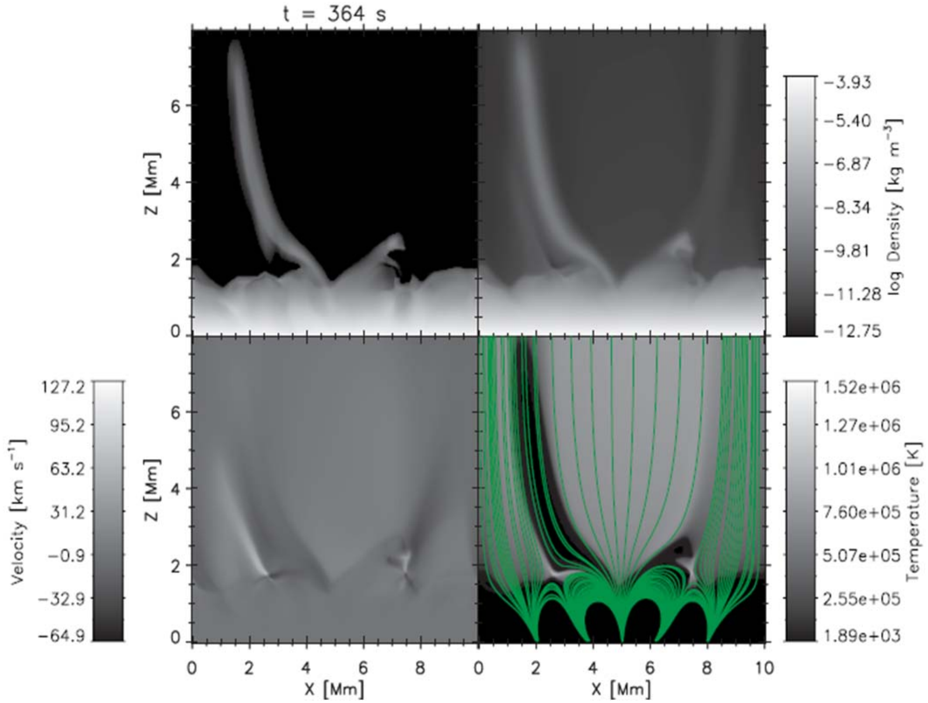

Chromospheric null points and HINODE driver

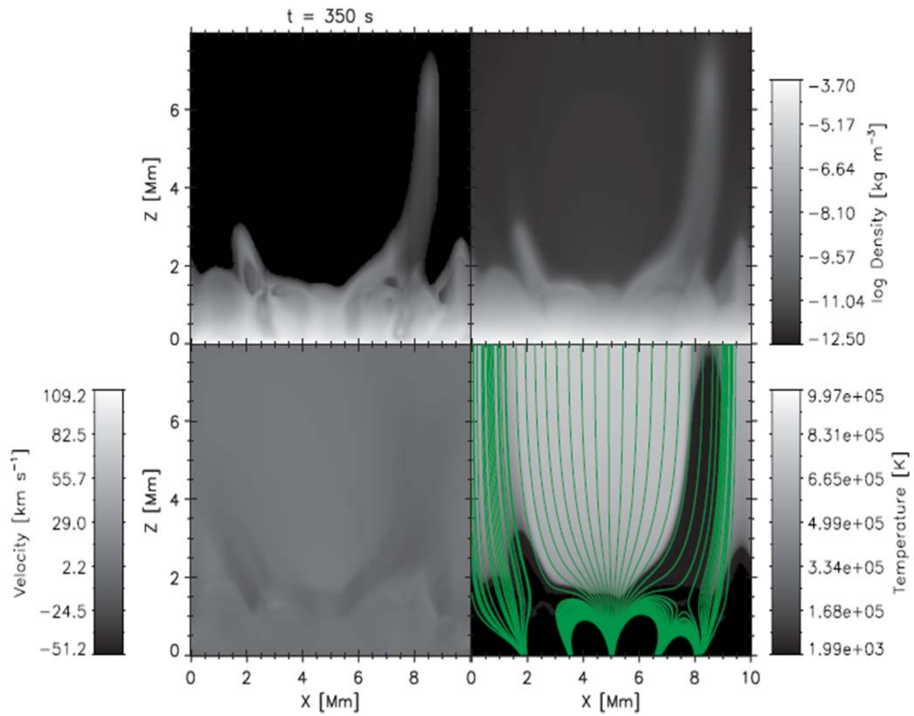

HEGGLAND, DE PONTIEU, & HANSTEEN
THE ASTROPHYSICAL JOURNAL, 702:1–18, 2009 September 1

Conclusions

- The solar chromospheric is an incredibly rich, dynamic and highly structured layer with complex poorly understood physics
- Chromospheric fine structures show a large diversity of physical and dynamic characteristics
- They are governed by flows reflecting the geometry and dynamics of the local magnetic field and play an important role in the propagation and dissipation of waves
- It seems that there are two distinctive populations of mottles/spicules
- Reconnection and p-mode leakage seem to be the most dominant driving mechanisms
- Chromospheric fine structures are important for maintaining the mass and energy budget of the solar corona
- Simulations of chromospheric fine structures are a new promising field. They do show some of the observed characteristics, however they are still far from the actual observed picture due to lack of detailed physics (e.g. detailed non- LTE radiative transfer, radiative cooling etc) and high-spatial numerical resolution

Thank you!

Special thanks to my partners in this “fine structure” journey:

- Georgia Tsiropoula (NOA, GR)
- Ioannis Kontogiannis (NOA & NKUA, GR)
- Petr Heinzel, Pavol Schwartz, Pavel Kotrc (Ondrejov Observatory, CZ)
- Pierre & Nicole Mein (Meudon Observatory, FR)